

<https://doi.org/10.3799/dqkx.2019.105>



造山型金矿研究进展:兼论中国造山型金成矿作用

王庆飞, 邓 军, 赵鹤森, 杨 林, 马麒谥, 李华健

中国地质大学地质过程与矿产资源国家重点实验室, 北京 100083

摘要: 造山型金矿指与大洋板块俯冲和陆块拼贴有关、产在汇聚板块边界变质地体内部或者边缘受韧—脆性断裂构造控制的, 成矿流体以低盐度 $H_2O-CO_2-CH_4$ 为主要特征的, 成矿深度(2~20 km)和温度(200~650 °C)及其相应的蚀变矿化组合有较大变化的系列金矿床。造山型金矿形成与超大陆聚合时限具有一致性。由于围岩类型和控矿构造多样性、地球化学特征具有多解性、金属源区和演化的不确定性以及成矿就位和物质起源的空间差距, 造山型金矿成因模式有以下两个主要观点。第一种为大陆地壳变质流体成因模式, 认为造山型金矿形成于造山作用同变质阶段, 并随岩石圈演化矿床的物质来源发生变化; 富含流体的释放由上地壳岩石绿片岩相到角闪岩相的进变质作用导致, 该过程中的黄铁矿向磁黄铁矿转变释放了大量的金, 这种模式被广泛运用于赋存在绿片岩相中的显生宙造山型金矿。然而越来越多的实例证实造山型金矿主要形成于峰期变质的退变质阶段或者与区域变质没有任何关系, 变质流体成因模式受到了强烈质疑; 与大陆地壳变质模式相对立的是幔源流体模式, 其认为流体起源于俯冲洋壳脱水或富集地幔再活化, 不同时代和地区的成矿流体具有一致性; 尽管该模式不符合传统的平衡条件下的相变原理, 但是基于幔源流体的存在及其浅部运移的大量观测, 初步认为成矿流体是在超临界和非平衡条件下完成了金属的幔→壳迁移。中国造山型金矿分布于江南造山带志留纪、天山—阿尔泰二叠纪、华北克拉通北缘三叠—侏罗纪、特提斯造山带二叠—侏罗纪、华南板块晚三叠世—侏罗纪、华北克拉通东南缘白垩纪、青藏高原及周缘古近纪等七大成矿带, 主要受到了显生宙不同时代造山作用的控制, 成矿时代晚于变质峰期, 重要成矿带大型矿集区(胶东、哀牢山、扬子西缘)的实例解剖均支持幔源流体成因模式。

关键词: 造山型金矿; 地幔流体; 变质流体; 构造控矿; 构造背景; 矿床。

中图分类号: P611

文章编号: 1000-2383(2019)06-2155-32

收稿日期: 2018-11-06

Review on Orogenic Gold Deposits

Wang Qingfei, Deng Jun, Zhao Hesen, Yang Lin, Ma Qiyi, Li Huajian

State Key Laboratory of Geological Processes and Mineral Resources, China University of Geosciences, Beijing 100083, China

Abstract: The orogenic gold deposits show features as follows: relation to oceanic plate subduction and terrane accretion, hosted by metamorphic massif along convergent plate boundaries, controlled by ductile to brittle shear zones, low salinity and $H_2O-CO_2-CH_4$ dominating ore fluid, wide formation depths varying from about 2 to 20 km and formation temperatures ranging within 200–650 °C, temperature-dependent alteration and ore mineral assemblages. Orogenic gold deposits formed coevally to the time of cycled convergences of supercontinents. Due to the diversity of wall rock types and ore-controlling structures, ambiguity of ore geochemistry, uncertainty of fluid and metal sources and their evolutions, and disparity between source regions and ore deposition locations, two distinct origin models were proposed for orogenic gold deposits. The first is metamorphic fluid model, in which the deposits formed in prograde metamorphism of orogeny with different source from evolving regional upper crust. The auriferous

基金项目: 国家重点研发计划项目(No.2016YFC0600307); 国家重点基础研究发展计划“973”项目(No.2015CB452606)。

作者简介: 王庆飞(1979—), 教授, 主要研究方向: 造山型金矿、特提斯演化与成矿。ORCID: 0000-0002-2883-692. E-mail: wqf@cugb.edu.cn

引用格式: 王庆飞, 邓军, 赵鹤森, 等, 2019. 造山型金矿研究进展: 兼论中国造山型金成矿作用. 地球科学, 44(6): 2155–2186.

fluid is considered to release from greenschist- to amphibolite-facies prograde metamorphism of upper crustal rocks, during which gold and other metals are liberated from transformation of pyrite to pyrrhotite. This model was universally applied to Phanerozoic orogenic gold deposit hosted by greenschist-facies terranes. However, it was recognized that most orogenic gold deposits formed in retrogression stage subsequent to peak metamorphism or without any spatial-temporal link to regional metamorphism, which challenged the metamorphic fluid model. Thus the mantle fluid model, which indicates that ore fluids for orogenic gold deposits are derived from devolatilization of subducted oceanic plate or fertile mantle, was proposed. Although the mantle fluid model is not compatible with the petrological diagram in phase equilibrium condition, the extensive proofs for the existence of mantle fluids and their appearance near surface support that mantle fluids are capable to transport to upper crustal levels under supercritical conditions and phase unequilibrium. The Chinese orogenic gold deposits are divided into seven gold belts: Silurian belt along Jiangnan orogen, Permian belt in Tianshan and Altay orogen, Triassic to Jurassic one along northern margin of North China craton (Solonker orogen), Triassic to Jurassic one within Paleo-Tethyan orogens, Jurassic one along southern margin of South China block possibly controlled by the Paleo-Tethyan closure, Cretaceous one along southern margins of North China craton, and Paleogene one in Tibetan Plateau and its margins. Orogenic gold deposits in China formed in Phanerozoic in association with various orogeny, with ore-forming ages post dating peak metamorphism. Case studies on gold districts in these belts, such as Jiaodong, Ailaoshan, and western margin of Yangtze craton, all favored the mantle fluid model.

Key words: orogenic gold deposit; mantle fluid; metamorphic fluid; structural control; tectonic setting; deposits.

0 引言

造山型金矿床指产于区域上各个时代变质地体中,在时间和空间上与增生造山或碰撞造山密切相关,形成于汇聚板块边界上的受到韧—脆性断裂控制的脉型和浸染型金矿床系列(Groves *et al.*, 1998).自造山型金矿提出以来,这一分类术语得到广泛的应用,它结束了以往对于剪切带金(或 gold-only)矿床纷繁的分类现状,对金矿成因研究和全球勘查工作起到重要作用.造山型金矿形成时代广,赋存深度宽,品位高并规模大,是全球金勘查的重要类型,其资源量占到全球金资源量的 30% 以上(Weatherley and Henley, 2013).中国自 2005 年起成为全球最大的金生产国(Groves *et al.*, 2018),对于造山型金矿的研究任务更为迫切.由于造山型金矿的地球化学特征具有多解性、金属源区和演化的不确定性以及成矿就位和物质起源的空间差距,因此成因一直存在争议.不同学者据此提出了不同的流体来源:(1)大陆地壳变质流体(Phillips and Powell, 2009, 2010; Tomkins, 2010),包括区域变质中的侧分泌(Saager *et al.*, 1982)、粒化作用(Fu and Toret, 2014)等;(2)大洋地壳俯冲相关或地幔流体(Goldfarb and Groves, 2015; Groves *et al.*, in press);(3)大气降水(Nesbitt, 1991);(4)岩浆—热液流体(Helt *et al.*, 2014)等.本文在对造山型金矿概念及连续成矿模式、成矿时代与构造背景、流体迁移沉淀及控制因素等方面研究进行综述基础上,深入剖析了变质流体成因模式和地幔流体成因模式的主

要依据和存在问题,进一步论述了中国造山型金矿成矿规律和成因模式.

1 基本概念与矿床模型

1.1 概念提出

早在造山型金矿提出之前,各国矿床地质学家就金矿类型提出了众多的分类方案(Phillips and Powell, 1993),包括根据金矿产出地区命名,如“Motherlode”型、“Bendigo”型、“Homestake”型和“Korean”型金矿;根据含矿岩石命名,如浊积岩型、板岩型、BIF 型、侵入岩型、绿岩带型以及火山岩型金矿;根据成矿温度压力命名,如“低温”(50~200 °C)、“中温”(200~300 °C)与“高温”(300~500 °C),该分类沿用至今;根据矿化样式命名,如置换交代(replacement)型、网脉(stockwork)型、脉(vein)型(Groves *et al.*, 1998; Morelli *et al.*, 2007; Goldfarb and Groves, 2015).由于分类纷繁复杂,一个金矿可以属于多个次级类型,不利于金矿床的成因研究(Safonov, 2010).针对此现象,不同学者对世界不同金矿床的研究,发现造山型金矿具有许多共同性质,尽管其围岩、时代和蚀变矿化特征有系统的差异,在大地构造背景、流体属性等方面却体现出较大的一致性;如其主要产于造山带内,与造山作用有密切成因联系,和岩浆作用没有明显成因联系等.这些特征明显不同于与火山岩有关的低温热液金矿、以沉积岩为围岩的卡林型金矿以及斑岩型和矽卡岩型等金矿类型.在系统阐述了造山型金矿

的概念及判别标准后(Kerrich and Wyman, 1990; Groves *et al.*, 1998),该类金矿逐渐引起国际矿床学家的广泛关注.

基于 Kerrich and Fyfe(1981)、Groves(1993)、Gebre-Mariam *et al.*(1995)和 Groves *et al.*(1998)等许多前人的研究,造山型金矿的概念被不同学者提出. Kerrich *et al.*(2000)提出此类金矿产生在俯冲晚期,高温变质流体沿大型剪切带灌入地壳,Au-HS 络合物在 $P-T$ 降到 300~400 °C 脱稳沉淀形成金矿. Kerrich and Wyman(1990)和 Kerrich *et al.*(2000)对数百至上千吨金产量的成矿带进行综合研究,并对比不同时代造山型金矿后,总结出该类金矿床的众多共同特征:(1)富金成矿带与增生造山作用紧密相关,主要形成于外汇聚超大陆旋回或内汇聚超大陆旋回外缘;(2)许多富金成矿带位于重要跨岩石圈构造附近或复杂的变质火山——深成、沉积地体边界附近;(3)在增生造山带的造山期内,成矿作用同步或滞后峰期变质作用及构造作用晚期;(4)大部分超大型造山型金矿成矿带位于绿片岩相变质地体中;(5)矿体主要赋存于脆—韧性断裂石英脉或蚀变岩中,

矿体形态、规模明显受构造作用控制,矿体呈平行斜列式脉群,以似层状、脉状产出;(6)绿片岩区域内的蚀变矿物共生组合主要以石英、碳酸盐、云母、绿泥石和黄铁矿为主;(7)矿床间具有相似地球化学特征,Au(As、Te、Sb、W、Bi、Mo、B)强富集,Cu、Pb、Zn、Hg 弱富集,成矿元素组合随深度变化,浅成为 Hg、Hg-Sb,中成为 Au-Sb-As-Te(图 1);(8)成矿流体主要为低盐度富水含碳流体,具有低盐度($\leq 6\%$), CO_2+CH_4 的含量为 5%~30%;(9)脆—韧性剪切带内,成矿流体压力从超静岩压力逐渐变化为次静岩压力;(10)动力变质岩在矿区内表现略具有分带性,而围岩蚀变的分带性不明显;(11)就单个矿床分析,矿脉系统可超过 2 km,蚀变和元素组合在垂向上延伸却无分带现象,或分带不明显.

Groves *et al.* (1998, 2003) 及 Goldfarb *et al.* (2001, 2005)综合大量代表性金矿床及成矿带的资料后发现,造山型金矿具有以下共同特征:(1)处于俯冲/活动大陆边缘压性应力场下,金成矿明显晚于峰期变质作用,太古代金矿经历后期变质叠加已经面目全非;(2)金矿床通常产出在变质的弧前和

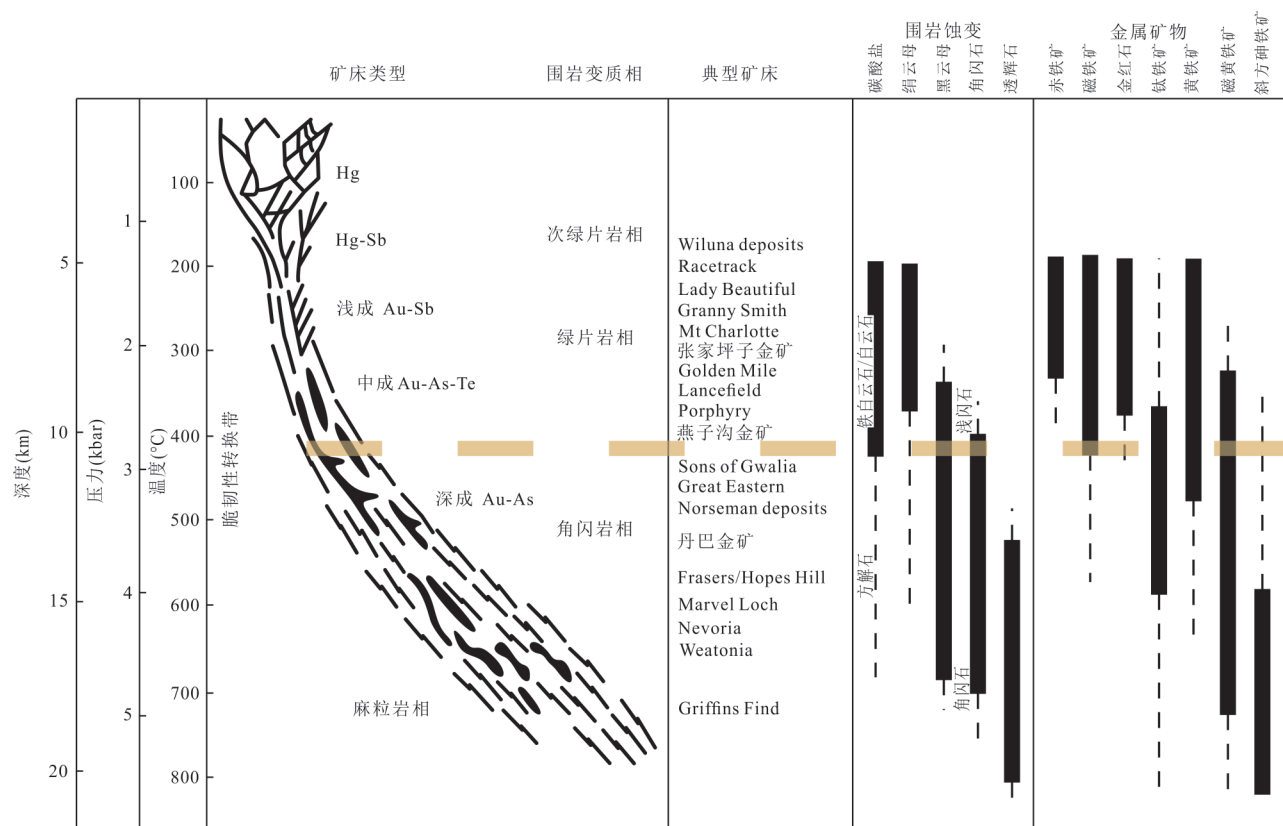


图 1 地壳连续成矿模式示意

Fig.1 Schematic distribution and characteristics of orogenic gold deposits in continuum model

据 Groves(1993)和 Groves *et al.*(1998)

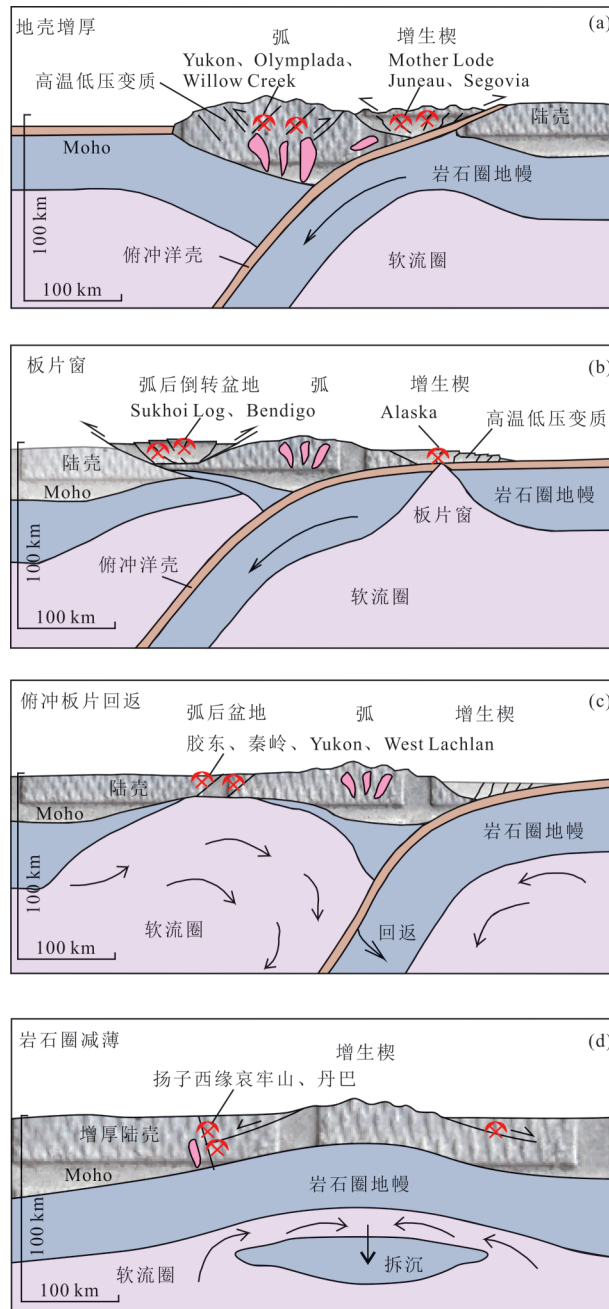


图 2 造山型金矿成矿大地构造背景

Fig.2 Geotectonic background for metallogenesis of orogenic gold deposits

a. 俯冲带上增生楔和岩浆弧带, 据 Goldfarb *et al.* (2005); b. 洋脊俯冲背景下的倒转弧后盆地, 据 Tomkins (2010); c. 俯冲板片回返与克拉通破坏, 据 Goldfarb and Groves (2015); d. 富集岩石圈地幔拆沉与大型穹窿, 据 Zhao *et al.* (2019)

弧后带内(图 2); (3) 基于蚀变类型组合及围岩组合, 这类金矿形成与围岩热平衡范围较宽, 由于成矿流体与围岩通常处于热平衡, 因此形成在高地热梯度带内的矿床少见; (4) K、S、CO₂、H₂O、Au 等元素及氧化物明显富集, As、B、Bi、Na、Sb、Te、W 等元素富集程度变化较大; (5) 超静岩流体以富 H₂O-CO₂-H₂S 和中低盐度为特征, 金沉淀机制可能为相分离或者围岩的硫化作用(Goldfarb *et al.*, 2005)。

1.2 地壳连续成矿

在认识到不同造山型金矿床具有共性的同时, 其内地质特征和矿床模型的差异性也被系统的研究, 地壳连续成矿是对造山型金矿床模型的基本概括. Groves *et al.* (1992) 对澳大利亚西部 Yilgarn 地块太古代岩金矿床长期研究发现, 大量矿床主要集中在绿片岩相和低角闪岩相变质岩中, 而西澳大利亚南克劳斯省产于角闪岩相和低麻粒岩相的两

个金矿床的成矿温度分别可达 500~550 °C 和 740 °C,围岩蚀变、矿物共生组合等方面都有别于低级变质区的金矿。Groves *et al.*(1992)基于金矿产出相带特征,初步提出地壳连续成矿模式,建议使用反映地壳深度的新术语,即“浅成带”(成矿深度 < 6 km, 150~300 °C)、“中成带”(成矿深度 6~12 km, 300~475 °C)、“深成带”(成矿深度 > 12 km, > 475 °C)来描述金矿床(图 1)。Groves(1993)进一步完善了太古代脉状金矿床的地壳连续成矿模式,认为从次绿片岩相到麻粒岩相的变质岩中均可以形成金矿床,并指出产在不同变质岩中的金矿床属于一组连续的同成因矿床组合,成矿温度变化在 180~700 °C,成矿压力至少在 1~5 kbar。需要强调的是,这种地壳连续成矿模式并非反映同一矿区的金矿化在垂向上的分布,而是集中反映了区域范围内一系列金矿床的分布特征。从地壳连续成矿模式中,浅部释放的流体与来自更深部的流体都可以形成相类似的矿床。

在地壳连续成矿模式中存在变质相由绿片岩相向角闪岩相、温度在 450~550 °C、蚀变矿物由绢云母向黑云母的重要过渡。浅成、中成和深成矿床的元素组合、矿石构造、围岩蚀变、金属矿物等均不相同,呈渐变过渡关系(图 1)。随着成矿深度(变质程度)增加,矿化构造样式由脆性向脆-韧性,再向韧性过渡。矿石构造由角砾型石英脉向平行片理和剪切交代型过渡;浅成矿床表现出梳状、皮壳状和晶洞充填状;中成矿床表现为块状和雁列状;深成矿床表现为粗粒脉状。

综上所述,尽管不同学者对于造山型金矿特征的认识不尽相同,其主体特征可以归结为:与大洋板块俯冲和陆块拼贴有关、产在汇聚板块边界变质地体内部或者边缘受韧-脆性断裂构造控制金矿,成矿流体以低盐度 H₂O-CO₂-CH₄ 为主要特征和成矿深度在 2~20 km 和温度在 200~650 °C 及其变化较大的蚀变矿物组合(图 1)。

2 成矿时代与背景

2.1 成矿时代

Goldfarb *et al.*(2001)和 Groves *et al.*(2005)通过大量金矿研究,系统总结了造山型金矿床形成的时间规律,发现在地质历史时期,造山型金矿主要形成时间存在 3 个峰期,分别为 2.80~2.55 Ga、

2.1~1.8 Ga 和 < 0.57 Ga(图 3)。前人研究发现这些造山型金矿的成矿峰期与陆壳增生速率的峰期和超大陆拼合峰期吻合较好(Barley and Groves, 1992; Goldfarb *et al.*, 2001)。例如,2.80~2.55 Ga 造山型金矿形成峰期与凯诺兰(Kenorland)超大陆的拼贴过程有关,此时形成的造山型金矿主要产于绿岩带内,包括 Yilgarn 克拉通的 Kalgoorlie、Superior 成矿省的 Timmins、Dharwar 克拉通的 Kolar、Zimbabwe 克拉通的 Kwekwe 等金矿(Goldfarb *et al.*, 2001)。2.1~1.8 Ga 造山型金矿形成峰期与哥伦比亚(Columbia)超大陆的拼贴过程有关(图 3),该时期形成的造山型金矿多发育于绿岩带和被动大陆边缘沉积岩系内,主要金矿实例包括西非的 Eburnean 造山带(如 Ashanti 金矿)、坦桑尼亚西南部的 Ubendian 造山带、Transamazonian 造山带位于圣弗朗西斯科克拉通、Trans-Hudson 造山带位于在北美(例如 Homestake 金矿)。< 0.57 Ga 造山型金矿成矿峰期与 Gondwana(冈瓦那)超大陆活动时期一致,大量造山型金矿分布在活动大陆边缘和古特提斯洋盆周缘,如澳大利亚东南部的 Bendigo-Ballarat 金矿集区、中亚造山带的 Muruntau 金矿集区、中国华北克拉通胶东金矿集区等(Goldfarb *et al.*, 2001)。

虽然罗迪尼亚超大陆活动期间(1.6 Ga~570 Ma)是陆壳增生速率的又一峰期,但是在近 1 000 Ma 的地球历史中缺乏确切的造山型金矿形成证据(图 3; Goldfarb *et al.*, 2001)。可见超大陆循环似乎不能很好的解释此时期造山型金矿空白现象,一些学者认为该时期保存的地质记录暗示全球处在克拉通内部裂谷发育时期及相关的非造山岩浆活动爆发时期,所以不宜形成造山型金矿(翟明国等, 2007),其他学者认为罗迪尼亚超大陆拼贴时期形成的造山型金矿床随陆壳重循环而缺失(Goldfarb *et al.*, 2001)。此外,Goldfarb *et al.*(2001)认为全球缺少 < 55 Ma 的大型造山型金成矿系统可指示中地壳岩石暴露至地表至少需要 ~50 Ma,然而目前青藏高原及其周缘已发现大型造山型金成矿系统,表明其上述观点有待商榷。

2.2 构造背景

造山型金矿主要沿活动大陆边缘带分布(Bierlein and Crowe, 2000; Goldfarb *et al.*, 2001, 2005; Bierlein *et al.*, 2006; Goldfarb and Groves, 2015),产于转换挤压或伸展构造环境。(超)大型造山型金矿形成的深部地球动力主要是俯冲事件中的软流圈

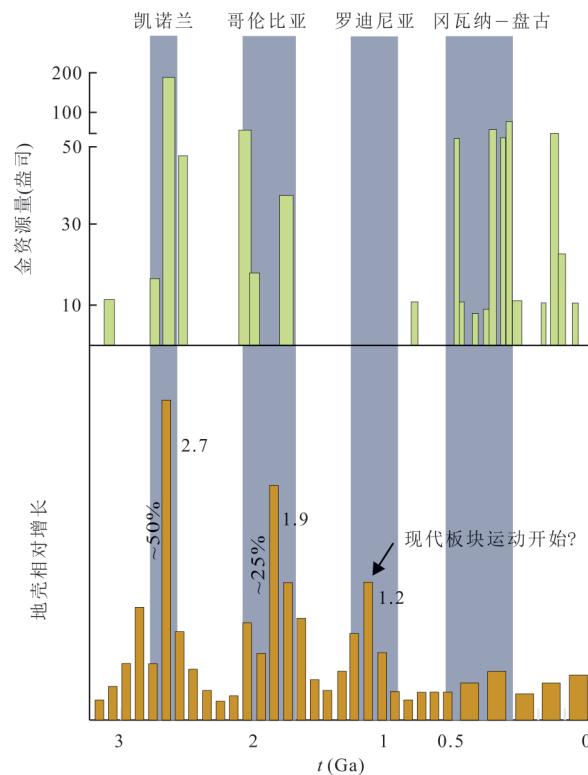


图3 全球造山型金矿形成时代分布及地壳生长模式统计

Fig.3 Statistics of formation ages for global orogenic gold deposits in earth history

据 Groves *et al.*(2005)

上涌等,模型包括:(1)弧后和增生楔伸展环境下的高温低压变质(图 2a),如北美 Yukon 和 Juneau 成矿带;(2)倒转弧后盆地和板片窗上增生楔的高温低压变质作用(图 2b),如俄罗斯远东 Sukhoi Log 和阿拉斯加-科迪勒拉;(3)俯冲板片回返引起克拉通破坏(图 2c),软流圈上涌促使成矿,如华北克拉通东南缘胶东成矿带;(4)地壳增厚后减薄(图 2d),软流圈上涌促使成矿,如扬子西缘丹巴金矿和哀牢山成矿带。Tomkins(2010)强调,单纯的伸展环境不利于造山型金矿形成,有利的大地构造背景是挤压或转换挤压,最有利的成矿环境是倒转的弧后盆地(含大量沉积岩堆积),成矿动力仍然是俯冲洋壳板片回返或板片窗引起的软流圈上涌,导致长英质下地壳重熔,引起区域变质,为高密度高通量热液的运移提供动能。

值得注意的是,世界上许多造山型金矿带的成因模式不适合经历多次板块碰撞和拼贴的中国大地构造环境。前者建立在大洋俯冲背景和构造体制由挤压向转换挤压的基础上,主要为单期造山模型,成矿时代以太古代和显生宙为主。中国则经历了复合造山和碰撞造山过程,成矿期主要处在挤压

到伸展的转换阶段,时代几乎均为显生宙,金矿形成晚于区域变质峰期,典型代表包括特提斯二叠-侏罗纪成矿带、华北克拉通东南缘白垩纪成矿带和青藏高原周缘古近纪成矿带等(翟裕生等,2009;Deng *et al.*,2014a,2015b)。

3 造山型金矿蚀变特征和构造控矿

3.1 热液蚀变

对于造山型金矿蚀变带的研究具有重要的经济和科学意义。成矿热液在上涌过程中遇到合适的围岩会发生蚀变反应,至少一部分金会因此从热液流体中卸载沉淀(Goldfarb and Groves, 2015)。在石英脉型金矿中,导流构造断裂控制了金的沉淀。蚀变反应发生在金矿体两侧;而在浸染状造山型金矿中,金呈浸染状分布在蚀变围岩中,金矿体和蚀变带在空间上叠加,金沉淀作用和水岩反应联系更紧密(MacKenzie *et al.*, 2007; Romer and Kroner, 2018; Sack *et al.*, 2018)。

热液蚀变发育在热液通道的两侧,走向及倾向上延伸至数百米,矿物组合变化小。靠近热液脉两

侧发育内蚀变带,热液活动强烈,发育以流体占主导的蚀变反应;而外蚀变带以围岩占主导,热液蚀变及矿化逐渐减弱.不同深度的造山型金矿围岩原岩含有不同的变质矿物组合,致使热液蚀变矿物组合及蚀变反应间存在差异(Bierlein and Maher, 2001).深成造山型金矿主要发育在前寒武角闪岩相或麻粒岩相变质的绿岩带中,以脉状金矿为主,金主要以自然金的形式与硫化物共生于石英脉中,两侧围岩蚀变带较窄,热液脉两侧发育硫化物(黄铁矿、雌黄铁矿为主)—石榴子石—黑云母—角闪石蚀变矿物组合,远端发育斜长石及角闪石矿物组合(Phillips and Powell, 2009, 2010; Tomkins and Grundy, 2009).而对于显生宙中浅成造山型金矿,热液蚀变带较为宽广(0.5~2.0 km),在超基性岩及变质浊积岩中均发育碳酸盐—绢云母(或铬水云母)—硫化物(以黄铁矿,毒砂为主)的热液蚀变.

热液蚀变过程中发生一系列蚀变反应,深成造山型金矿中,绿岩带中角闪石及斜长石被黑云母、阳起石、辉石和钾长石等矿物交代(Kolb *et al.*, 2015);而对于中浅成造山型金矿,绿片岩变质相的浊积岩围岩中绿帘石及绿泥石被热液碳酸盐及绢云母交代,沉积型绢云母被热液绢云母交代(Christie and Brathwaite, 2003; MacKenzie *et al.*, 2007).云南哀牢山镇沉金矿发现磁铁矿颗粒被黄铁矿交代并有碳质颗粒析出;煌斑岩及石英斑岩中的黑云母或金云母斑晶蚀变成碳酸盐及绢云母,并有金红石、磷灰石颗粒延云母节理分布(Li *et al.*, 2019b).

3.2 控矿构造类型

控矿构造的几何学样式在造山型金矿研究内达成共识(Groves *et al.*, 2018).构造几何学研究发现,褶皱转折端和层间滑脱带通常是矿体赋存的有力部位,例如Bendigo金矿(图4a; Cox *et al.*, 1991);对于剪切带或断裂控制的造山型金矿,断裂弯曲转折端(bend;图4b; Yang *et al.*, 2018a)、剪切带张性或压性衔接部位(jog;图4c; Hodkiewicz *et al.*, 2009)、里德尔剪切派生裂隙以及不同断裂相交点常常是矿体出现的主要场所.此外,由于花岗质侵入体的存在,在侵入体与其他岩性接触部位的最大主应力方向发生明显偏转,从而导致岩性接触带具有异常低的最小主应力,易于流体侵入,因此花岗质侵入体形成的岩性接触带是造山型金矿产出的重要部位(Groves *et al.*, 2018).大型、超大型金矿形成的必要条件之一是从源区运移大量成矿流体(Vearn-

combe, 1998),上述不同的构造几何学样式是易于流体聚集的场所.加拿大Superior省和澳大利亚Yilgarn克拉通金矿分布和剪切带具有明显相关性,指示这些剪切带是大量流体运移的通道(Eisenlohr *et al.*, 1989; Groves *et al.*, 1992); Weinberg *et al.* (2004)研究发现剪切带或断裂转折端偏离主断裂平均走向高达 $10^{\circ}\sim 25^{\circ}$,这种产状变化部位是矿体富集的有力部位(图4d);宏观观察和地震数据表明这些“流体通道”是地壳尺度的,长达几百公里,长达25 km(Groves *et al.*, 1992; Drummond *et al.*, 1993).另外,在Yilgarn克拉通北东部Yandal绿岩带内以及我国的重要造山型金矿集中区,区域尺度剪切带内并无蚀变和矿化,矿床受距剪切带几公里远的脆性断裂控制(Vearncombe, 1998; Tripp and Vearncombe, 2004);因此,在部分情况下,区域尺度(一级)构造通常为成矿流体的运移通道,而矿床尺度(二级)剪切带或断裂控制造山型金矿的产出(Groves *et al.*, 2018).

3.3 传统构造控矿分析

传统的矿田构造的研究过程通常包括划分构造变形期次,分析不同期次构造运动学、几何学特征,反演主应力方向,解释构造动力学成因及相应成矿作用(Carrier *et al.*, 2000; Blenkinsop and Doyle, 2014; Fridovsky, 2017; Lebrun *et al.*, 2017; Bell *et al.*, 2018).例如Lebrun *et al.* (2017)研究西非Siguiri金矿集区时发现,其构造演化可分为四个阶段:SN向挤压形成W-NWW向褶皱;E-W到ENE-WSW向挤压,形成SN向构造要素;NNW-SSE向转换伸展,控制金矿化;NW-SE向挤压,形成NNE-SSW韧性劈理.由于不同造山型金矿控矿构造演化和运动学差异较大,虽然其对单个矿床矿产勘查具有指导意义,然而难以总结统一的模式;更为重要的是其忽略了成矿流体和构造之间的相互作用.

3.4 流体对构造的反馈

众所周知,应力是岩石变形、破裂的主要驱动力,然而流体的注入会对围岩产生流体压力,其在岩石变形、破裂过程中同样扮演重要的角色(Sibson *et al.*, 1988; Sibson, 1996, 2001; Cox, 2010, 2019).在一定的地壳深度,空隙流体因子(λ_v)可用来描述流体压力级别($\lambda_v = \text{流体压力}(p_f) / \text{岩石垂向应力}(\sigma_v)$)在经历绿片岩相以上变质作用的地震带中,静水压力下接近0.4,而在静水压力下 λ_v 接近1.0,超静水压力下 λ_v 介于0.4和1.0,流体压力随着深度的增加而增

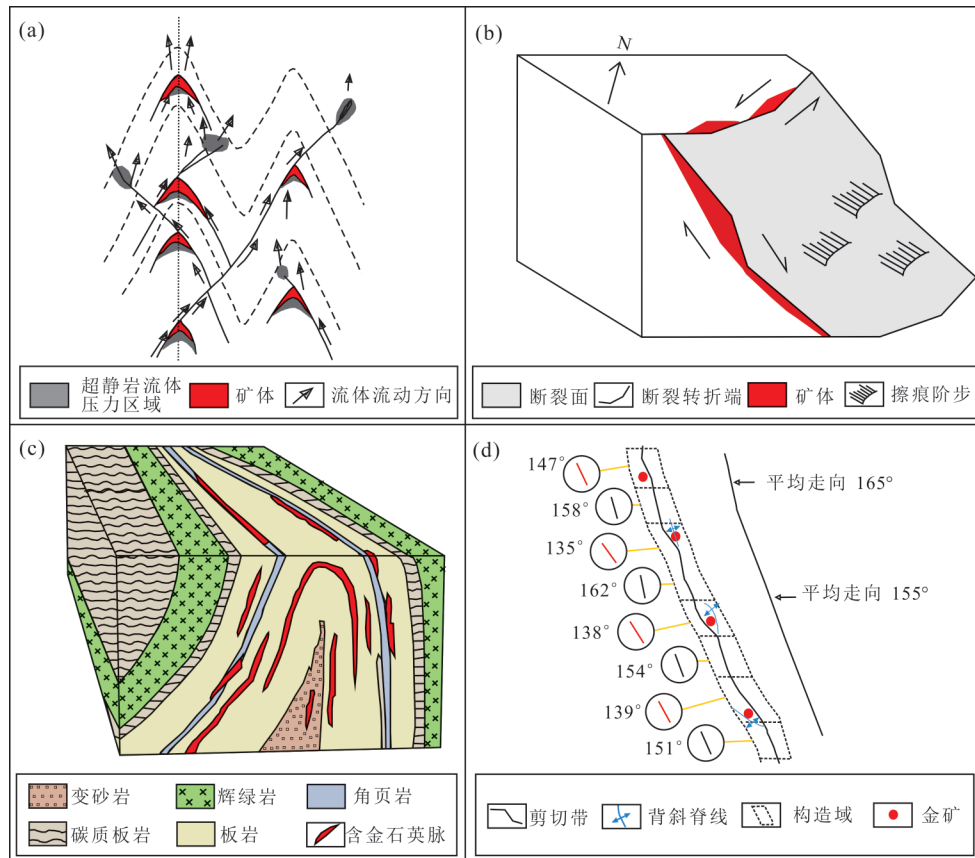


图4 造山型金矿构造控矿示意

Fig.4 Schematic diagrams of structural control on orogenic deposits

a. 褶皱转折端控矿示意图, 据 Cox *et al.* (1991) 修改; b. 断裂弯曲转折端控矿示意图, 据 Yang *et al.* (2018b) 修改; c. 剪切带张性或压性衔接部位控矿示意图, 据 Hodkiewicz *et al.* (2009) 修改; d. 剪切带或断裂转折端控矿, 据 Weinberg *et al.* (2004) 修改

加(图 5a; Sibson, 2004; Cox, 2010, 2019). 流体压力和差应力($\sigma_1 \sim \sigma_3$)共同决定岩石产生的破裂样式, 当流体压力较小, 差应力大于等于 5.7 倍岩石抗张强度时, 岩石主要受应力驱动产生剪裂隙; 当流体压力较大, 差应力小于等于 4 倍岩石抗张强度时, 岩石将产生张裂隙; 当流体压力较大, 差应力介于 4 倍和 5.7 倍岩石抗张强度时, 岩石将产生混合的张剪裂隙(图 5b; Sibson, 2001, 2004; Streit and Cox, 2001; Cox, 2010, 2019). 应力和流体驱动的裂隙的张开闭合, 流体压力周期性改变, 称为“地震泵”原理(Sibson *et al.*, 1988; Sibson, 1996, 2001), 该原理已经广泛地用于解释造山型金矿成因(Kolb *et al.*, 2005). 由于流体的存在, 在韧性变形区仍然可以形成断层和矿脉, 其突破了传统的断裂和矿脉通常形成于脆韧性剪切带及以上的观点(Sibson, 2004).

流体影响构造活动的另一主要因素为水岩反应(Yang *et al.*, 2018a), 水岩反应是造山型金矿金沉淀的主要机制之一(Kolb *et al.*, 2000; Hodkiewicz *et al.*, 2009; Williams-Jones *et al.*, 2009).

水岩反应过程中, 矿物溶解可形成大量孔隙度, 而矿物沉淀导致孔隙度闭合, “硬”矿物(如角闪石、长石)的溶解, “软”矿物(如云母、绿泥石)的形成通常引起岩石软化, 导致岩石更易发生破裂(图 5c; Wintsch *et al.*, 1995; Sausse *et al.*, 2001; Yasuhara *et al.*, 2006). 研究表明花岗岩钾长石化蚀变前后摩尔体积增加 9%, 而随后与金密切相关的绢云母化将导致其摩尔体积下降 8%~57%, 体积的改变控制围岩孔隙度形成, 而矿质沉淀导致孔隙度闭合(图 5d), 这些热液蚀变导致花岗岩岩石软化, 软化后岩石与原岩相比更易发生破碎(图 5c; Yang *et al.*, 2018b). Mernagh and Bierlein(2008)通过化学模拟进行质量迁移计算, 发现在高温条件下, 流体与含金沉积岩或者绿片岩发生反应达到化学平衡状态时, 流体含有最高的金含量. 可见, 水岩反应不仅可以引起岩石软化, 导致岩石易于破裂, 其反应后形成含有高的金含量的流体也是形成金矿的必要条件.

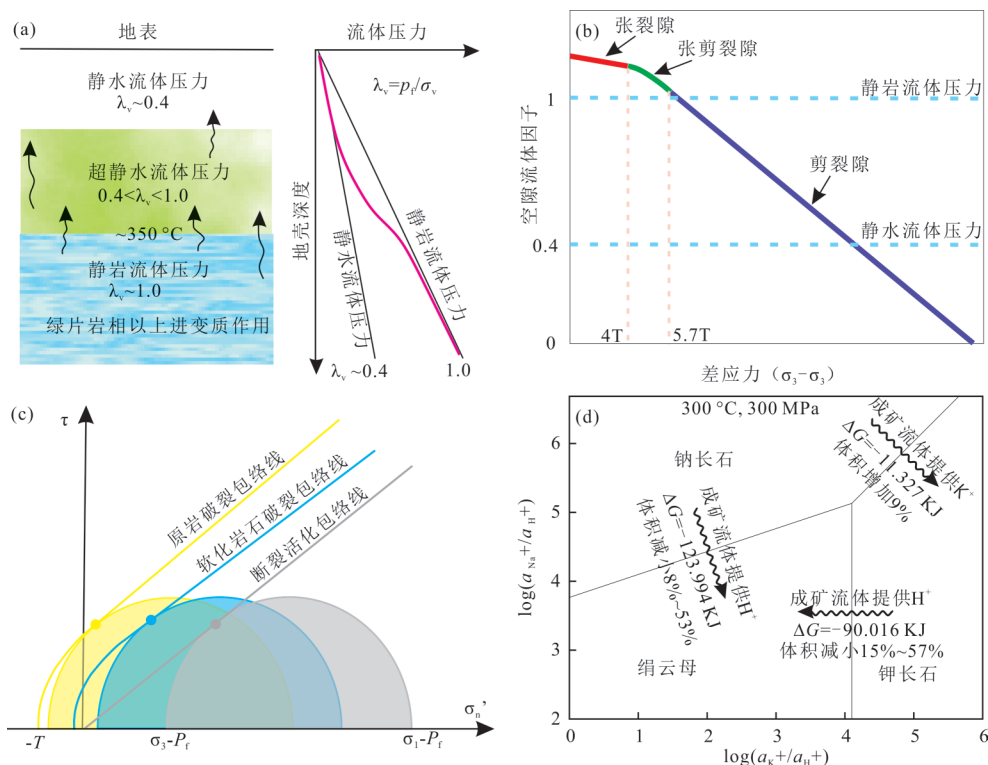


图 5 (a)假定的绿片岩相以上进变质区域流体压力剖面;(b)完整岩石脆性破裂模式图;(c)格里菲斯-库伦岩石破裂准则;(d) $\log(a_{K^+}/a_{H^+})$ vs. $\log(a_{Na^+}/a_{H^+})$ 相图

Fig. 5 (a) Hypothetical fluid-pressure profile through the carapace to a region undergoing prograde metamorphism defining the seismogenic zone; (b) schematic illustration of a brittle failure mode diagram for intact rock failure; (c) composite Griffith-Coulomb failure envelopes for intact rock (long dash line) with tensile strength; (d) isothermal-isobaric $\log(a_{K^+}/a_{H^+})$ vs. $\log(a_{Na^+}/a_{H^+})$ diagram

图 a. λ_v 为流体压力因子, $\lambda_v = p_f(\text{流体压力})/\sigma_v$ (岩石垂向应力) (据 Sibson, 2004); b. 展示流体因子和差应力改变可诱发岩石破裂. 差应力大于等于 5.7 倍岩石抗张强度时, 岩石产生剪裂隙; 差应力小于等于 4 倍岩石抗张强度时, 岩石将产生张裂隙; 差应力介于 4 倍和 5.7 倍岩石抗张强度时, 岩石将产生混合的张剪裂隙 (据 Cox, 2019); c. 黄色、蓝色、灰色颜色代表花岗岩原岩、软化花岗岩、断裂活化的莫尔圆和包络线 (据 Sibson and Scott, 1998); d. 指示蚀变过程矿物转化, 据 Yang *et al.* (2018b) 修改; 黑色波浪线代表胶东新立金矿蚀变反应路径, G 代表反应前后吉布斯自由能变化

3.5 构造-矿化网络尺度不变性

热液成矿过程是一个复杂的过程, 符合分形几何学原理, 表明在无序的、不规则的矿床几何学背后, 存在潜在规则的样式, 这种样式具有尺度不变性, 可以用分形数学解析和刻画 (Gumiel *et al.*, 2010; Haddad-Martim *et al.*, 2018; Munro *et al.*, 2018). Haddad-Martim *et al.* (2018) 研究世界著名的 Carajás 成矿省中铁铜金矿床 (IOCG) 时发现, 区域尺度、矿体尺度和显微尺度控矿裂隙几何学具有尺度不变性; 由于构造是控制成矿流体流动的主导因素, 因此这种尺度不变性可归因于构造控制 (Haddad-Martim *et al.*, 2018). 在造山型金矿中, Yang *et al.* (2015) 通过对胶东新立金矿围岩蚀变、金品位空间分布及分形特征研究, 认为这种控制金品位空间

分布的岩石渗透性的尺度不变性是通过自组织机制实现的. Yang *et al.* (2018b) 借助金品位多重分形和赫斯特指数研究, 进一步定量地厘定了金品位的孔隙度网络空间结构, 研究发现在相似的构造部位和蚀变矿化带内发育正相依和反相依的孔隙度网络结构, 其可解释为构造-水岩反应联合控制的差异的岩石渗透性网络结构.

4 造山型金矿成因模式

4.1 大陆地壳变质流体成因模式

4.1.1 提出与依据 大多数学者认可的造山型金矿成矿流体应该为变质热液流体 (Goldfarb *et al.*, 2005; Large *et al.*, 2007, 2011; Steadman and Large, 2016).

Pitcairn *et al.*(2006)研究 Otago Schists 金矿时发现变浊积岩进变质过程中释放 Au、As、Bi、Sb、Te、W 等成矿元素,在浅部地壳形成金矿。Large *et al.*(2007, 2009, 2011)针对黑色页岩容矿的金矿床,通过黄铁矿和磁黄铁矿原位微量元素研究建立了两个阶段金富集模式,即早期沉积或成岩期,金及其他微量元素进入含砷黄铁矿中;晚期在绿片岩相或更高级别变质作用下,黄铁矿转化为磁黄铁矿释放 S、Au 及其他成矿元素,在这种变质条件下绿泥石转化为黑云母释放流体(Tomkins, 2010; Finch and Tomkins, 2017)。

据此,一些学者相应地提出成矿流体和金属来源均为中上地壳岩石变质的“变质流体成因模式”(Phillips and Powell, 2009, 2010, 2015; Tomkins and Grundy, 2009; Tomkins, 2010)。该模式主要认为,在绿片岩相到角闪岩相的进变质过程中,含水和碳酸盐的绿片岩相岩石(特别是变基性岩)脱水作用是造山型金矿的流体来源(图 6a, 6b)。Zhong *et al.*(2015)通过模拟后提出:①黄铁矿向磁黄铁矿的转化释放的 S 很少,因为这些 S 多与绿泥石和云母中的 Fe 反应生成磁黄铁矿;②绿泥石变质过程生成水,因而能从源岩(比如富 S 泥质岩)中提取大量 Au;③绿泥石大量脱水的主要温度区间是 500~650 °C(图 6c)。变质流体成因模式认为,生成的变质热液流体周期性的沿深大断裂上升(Sibson *et al.*, 1988),向上进行数公里的运移到地壳更浅部成矿,形成于中温(200~450 °C)环境。金的沉淀发生在绿片岩相条件下或者是脆-韧性过渡的地壳深度以上,这个深度一般是在中上地壳地震带部位。

4.1.2 原理 (1)变质脱水。随着进变质过程中温度压力的升高,脱水反应表现为沸石、碳酸盐、绿泥石和泥质矿物等含水矿物组合转化为含水少或不含水组合并脱水(Bucher and Grapes, 2011)。沸石类脱水反应包括:浊沸石→斜钙沸石+水;斜钙沸石→葡萄石+高岭石+石英;方沸石+石英→钠长石+水。如果 CO₂ 存在,脱水反应则为:浊沸石+CO₂→方解石+高岭石+石英+水。

与绿泥石向云母转化脱水有关的典型反应式(Bucher and Grapes, 2011)例如:

① 绿泥石带→黑云母带

Chl(绿泥石)+Phn(多硅白云母)=Bi(黑云母)+Ms(白云母)+SiO₂+H₂O,

3Chl+6Ms=6Bi+3Chl(富铝镁)+14SiO₂+H₂O,

H₂O,

Stp(黑硬绿泥石)+Phn=Bi+Chl+SiO₂+H₂O.

② 绿泥石+黑云母带→铁铝榴石带

Chl(Fe₉Al₆Si₅O₂₀(OH)₁₆) + 4SiO₂ = 3Gt(Fe₃Al₂Si₃O₁₂, 石榴石)+8H₂O,

Cld(硬绿泥石)+Bi=Gt+H₂O,

Fe-Cld+Ann(羟铁云母)=Alm(铁铝榴石)+H₂O.

③ 绿泥石+黑云母带→十字石带

Chl+Ms=St(十字石)+Bi+SiO₂+H₂O.

(2)变质脱硫。伴随含水流体的生成,为保持体系 H₂O、H₂S、SO₂、O₂ 的化学平衡(Tomkins, 2010),S 也从黄铁矿中提取并释放到流体中(Connolly and Cesare, 1993):

FeS₂+H₂O=FeS+H₂S+1/2O₂ 或 3FeS₂+2H₂O=3FeS+SO₂+2H₂S.

如果体系中有 C(如碳质泥岩、板岩)存在,则可有 CO₂ 生成(Connolly and Cesare, 1993): 2FeS₂+2H₂O+C=CO₂+2H₂S+2FeS.

(3)脱碳酸盐化。当然,CO₂ 还有许多其他途径生成,比如脱碳酸盐化(Bucher and Grapes, 2011):

Calcite + Quartz=Wollastonite(Ca₃(Si₃O₉)) + CO₂,

Margarite + 2Quartz + Calcite=2Anorthite + CO₂+H₂O,

11Dolomite + Tremolite=13Calcite + 8Forsterite + 9CO₂+H₂O,

8Quartz + 5Dolomite + H₂O=Tremolite + 3Calcite+7CO₂.

变质脱水、脱硫和脱碳酸盐化是生成含挥发分流体的基本反应,这些反应广泛发生在分布广泛的中上地壳绿片岩带内。Elmer *et al.*(2006)计算出该过程可以释放的流体占镁铁质火山岩岩石体积的 5%, 足够形成大型金矿床(Phillips and Powell, 2010)。

4.1.3 适用性 对于全球众多产于绿片岩相地体里的造山型金矿,变质流体成因模式显得适用。变质流体成因模式有实验岩石学和变质脱流体理论的支持,但它却不能解释许多高温深成的太古代和显生宙金矿床,主要包括如下方面:

(1)成矿时代。造山型金矿研究的一个基本问题在于这些矿床是形成于变质峰期或峰期之后

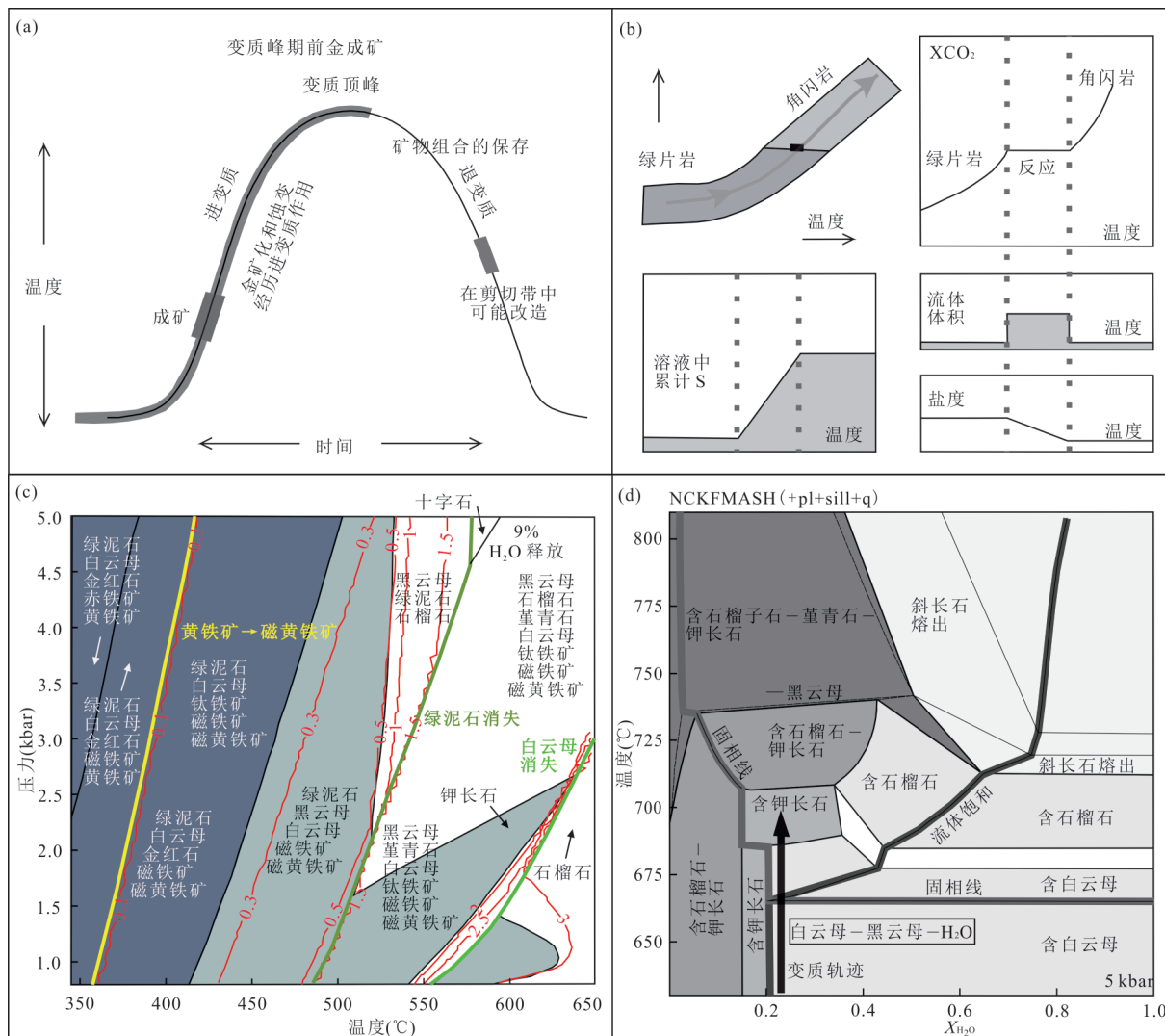


图 6 变质流体成因模式示意图

Fig.6 Schematic graphs for metamorphic fluid model

a. 变质峰期前成矿, 据 Phillips and Powell (2009); b. 绿片岩相一角闪岩相进变质脱水, 据 Phillips and Powell (2010); c. 500~650 °C 为主要脱水区间, 据 Zhong *et al.* (2015); d. 变质体系有水 > 650~700 °C 情况下引起部分熔融, 据 Phillips and Powell (2009); NCKFMASH 代表着 Na₂O - CaO - K₂O - FeO - MgO - Al₂O₃ - SiO₂ - H₂O 初始组分体系

(Groves *et al.*, 1998; Goldfarb *et al.*, 2005) 还是形成于变质峰期之前(可能遭受之后变质作用的叠加; Phillips and Powell, 2009, 2010; Tomkins, 2010). 前者支持一个外来深源流体(Goldfarb and Groves, 2015); 后者认为含金流体来自沉积岩系的绿片岩相一角闪岩相变质作用脱水. Goldfarb *et al.* (2005) 和 Goldfarb and Groves (2015) 统计认为大部分造山型金矿都显示为峰期或峰期后成矿. 这一结论是基于西澳 Yilgarn、加拿大 Abitibi、印度以及南非等矿床的资料 (Knight *et al.*, 1993, 2000; Dziggel *et al.*, 2010; Kolb *et al.*, 2015), 证据包括成矿和变质年龄对比、围岩蚀变特征、矿脉与围岩的穿切关系等, 比

如蚀变矿物组合往往叠加在围岩顶峰变质矿物组合之上. New Consort、Renco、Hutti、Hira Buddini、Navachab、Nevoria 和 The Granites 等矿床都支持变质峰期之后成矿的观点 (Kolb *et al.*, 2015).

Stüwe (1998) 和 Phillips and Powell (2010) 用 “Deeper-Later” 模式解释变质峰期与成矿年龄的问题, 其认为在受抬升剥蚀的造山带中, 地壳越深部位到达变质峰期比地壳浅部要晚, 因此深部源区形成的流体就位成矿的时代可能表现为晚于围岩变质峰期. 但 Groves *et al.* (in press) 认为绿片岩相矿物变质反应普遍表现出微观流体运移, 结合围岩中的无矿石英脉, 表明已有变质流体生成难以解释, 而

后突然出现成矿的高密度含金流体.许多特别的显生宙造山型金矿,例如胶东成矿带(Deng *et al.*, 2011, 2015a)成矿在~120 Ma,而区域高级变质及相应的变质脱水作用发生在2 000 Ma之前.这些矿床用“Deeper-Later”模式无法解释.哀牢山成矿带最新研究结果也表明,金矿化晚于剪切活动和峰期变质(Gao *et al.*, 2018).

(2)深成矿床.许多产在角闪岩相—麻粒岩相中的太古代金矿床,其最大形成深度在15~20 km (Groves *et al.*, 1998, 2005).如果在麻粒岩相变质条件下可发生金成矿作用,那么必然有来自更深的流体参与了成矿.若该推论正确,则绿片岩相向角闪岩相转变过程释放的流体,对麻粒岩相金矿的形成没有任何贡献.变质脱流体模式认为造山型金矿只可能形成于变质峰期之前的中温环境,矿床形成后可能会继续经历进变质作用,甚至是部分熔融的过程(图6d).基于Griffin's Find矿区内的石榴子石黑云母片麻岩在峰期变质作用经历过部分熔融,形成的熔体可以削减应变,使得早期形成的矿化脉体不发生变形(Tomkins and Grundy, 2009).

变质流体成因模式强调这类形成于高级变质相(角闪岩相到麻粒岩相)中的深成金矿床,原来都是绿片岩相变质热液矿床,只是在后来遭受了更高级变质(变形)作用的叠加(Phillips and Powell, 2009).但Kolb and Meyer(2002)、Kolb *et al.*(2005)和Sarma *et al.*(2011)在对印度的超大型Hutti和Kolar金矿床研究后认为,这类前寒武深成造山型金矿中的少数确实遭受了变质叠加,但却是在后一次造山事件中.世界范围内已陆续发现许多显生宙高温深成金矿,包括加拿大Meguma金矿带(Kontak *et al.*, 1990)、法国French Massif金矿带(Bouchot *et al.*, 2005)以及中国扬子西缘的产在角闪岩相中的丹巴金矿(Zhao *et al.*, 2019)等.这些矿床成因研究也表明,成矿发生在高级变质温度压力条件下,并未受到后期变质叠加.

(3)成矿物质来源.深成金矿床高温成矿特点及其晚变质成矿时限,使得成矿流体不太可能来自围岩沉积岩系的变质,反之需要来自深部的外来成矿流体.Goldfarb *et al.*(2001)根据全球众多矿床的资料归纳出:前寒武造山型金矿的成矿物质源区主要为变质火山岩,从超基性到长英质均有,以镁铁质为主(Tang and Santosh, 2018);显生宙造山型金矿的物质来源则主要为变质沉积岩,主要为浊积岩或复

理石建造(Steadman *et al.*, 2013).尽管Pitcairn *et al.*(2006)针对新西兰Otago Schists金矿物源岩石实验结果表明,和成矿相关的金属元素能通过变质沉积岩系在地壳深部的变质作用而被提取出来,然而前寒武纪造山型金矿的主要围岩—镁铁质岩却不能释放大多数造山型金矿床的常见金属元素As(Pitcairn *et al.*, 2015).

造山型金矿混合的稳定同位素和放射性同位素特征也指示广泛的流体通道和深部来源(Ridley and Diamond, 2000; Standish *et al.*, 2014).例如Browning *et al.*(1987)、McNaughton *et al.*(1993)以及LaFlamme *et al.*(2018)在对西澳Yilgarn克拉通超大型东部金矿田的研究中发现,其硫—铅同位素年龄和组成反映了从基底岩石到上地壳岩石的特征(Selvaraja *et al.*, 2017),这就否定了中上地壳岩石变质流体作为造山型金物质来源的成因模式.

4.2 地幔流体成因模式

4.2.1 提出及观点 角闪岩相—麻粒岩相形成的前寒武纪和显生宙高温深成金矿(Kolb *et al.*, 2015; Zhao *et al.*, 2019)需要一个外来深源成矿流体.相似的是,华北克拉通东南缘白垩纪造山型金矿(Deng *et al.*, 2015c; Goldfarb and Groves, 2015),以及墨西哥Megashear剪切带中的第三纪造山型金矿(Goldfarb *et al.*, 2007),其围岩在成矿几百到两千个百万年之前就已经经历了与伸展构造和变质核杂岩有关的高级变质作用.在这些显生宙成矿带里,地壳岩石从经历了区域变质作用(温度至少在500~600 °C)的地壳深度抬升剥露到地表.这些岩石早已脱水和脱挥发分,其黄铁矿基本已转变为磁黄铁矿,因而缺乏足够的Au和S形成有规模意义的金矿床(Goldfarb and Groves, 2015).由于变质流体成因模式无法解释这类金矿床(成矿带),应运而生的是为解决这类矿床成因问题的“地幔流体成因模式”.

基于不同造山带大地构造和矿床地质的研究,不同学者提出了不同的与俯冲有关的地幔流体模式,可归纳为三种:俯冲洋壳脱水与流体回返模式(Peacock, 1990; Sibson, 2004; Peacock *et al.*, 2011)、克拉通破坏富集地幔脱气模式(Goldfarb and Santosh, 2014; Deng *et al.*, 2015c)和岩石圈拆沉富集地幔脱气模式(Zhao *et al.*, 2019; Wang *et al.*, in review).

4.2.2 俯冲洋壳脱水与流体回返 在弧前地带,俯冲板片脱水产生的流体沿着板片与地幔楔边界向上

运移是被广泛认识到的地质现象(Peacock, 1990; Wyman and Kerrich, 2010; Hyndman *et al.*, 2015). 俯冲板片脱挥发分,同时含挥发分含金流体沿着俯冲板片向上移动到弧前地区,最终进入地壳浅部地震带沉淀成矿(Sibson, 2004; Peacock *et al.*, 2011)(图7a). 该模式在弧前地区成功识别,例如 Otago 地区(Breeding and Ague, 2002). Kawano *et al.*(2011)认为在小于 100 km 低于 650 °C 的板片深度下,地幔楔边缘底部高度剪切的蛇纹岩层含有特定渗透带,该渗透带为板片脱水提供储存空间. 大洋板片和上覆含黄铁矿沉积物释放的流体,在弧前地幔增生楔一旦水饱和后就会开始移动(Katayama *et al.*, 2012). 生成的超高压流体将向上运移(Sibson, 2013),灌入岩石圈规模尺度的断裂带,最终在地壳浅部次级构造带中成矿.

4.2.3 克拉通破坏富集地幔脱气 Goldfarb and Santosh(2014)在研究胶东金矿时提出,由于围岩早在约 2 000 Ma 前就已经经历高级变质作用,唯一可行的成矿流体来自地壳以下富集地幔脱气(图7b). 在这个模式中,俯冲洋壳板片上覆的富 Au 和其他相关元素的含黄铁矿沉积物非常重要,因为它是含金流体 Au、S、C、O、H 等元素最终的物源(Chen *et al.*, 2008; Large *et al.*, 2009, 2011; Steadman *et al.*, 2013). 125 Ma 以前受到破坏的华北克拉通以下的太平洋板块俯冲角度已很难确定,但俯冲板片释放的流体可能通过郯庐断裂向上运移并进入次级断裂成矿. 另一种可能的机制是,俯冲板片释放的流体使地幔楔边缘蛇纹石化并富集 S、C、Au 等元素,并可以保存在富集地幔楔中数十个百万年(Groves and Santosh, 2015, 2016),随后大约 125 Ma 的克拉通破坏和软流圈上涌促使富集地幔楔脱气并释放成矿流体. Wyman *et al.*(2008)和 Seno and Kirby(2014)认为,这类流体的释放最可能由板片失稳、俯冲停止和板片窗等过程引发,地幔楔脱水可发生在俯冲板片停止后 10~25 Ma. 这些过程与同时代古太平洋板块应力场由挤压过渡到转换挤压契合(Goldfarb *et al.*, 2001, 2007, 2014).

4.2.4 岩石圈拆沉富集地幔脱气 Hronsky *et al.*(2012)认为,在同碰撞或之前俯冲事件中不均一交代富集的岩石圈地幔可作为造山型金矿统一的物质来源. 在特提斯二叠—侏罗纪成矿带东缘的扬子克拉通西缘即存在~830 Ma 俯冲形成的交代富集的岩石圈地幔(Zhou, T.H. *et al.*, 2002b; Zhou, M.F. *et al.*,

2008). 该带区域花岗岩由后碰撞 230~200 Ma 的 I 型和埃达克质演化为碰撞后 210~180 Ma 的 A 型和 S 型,后者与强烈壳幔作用和岩石圈伸展一致. 岩石圈拆沉或其他相似过程被认为是引起该区域早侏罗岩石圈伸展的深部机制(Zhang *et al.*, 2007). 为岩石圈伸展提供了更确切证据的是扬子西缘 >1 000 km 的形成于 180~160 Ma 的穹隆带(Zhou *et al.*, 2002a, 2008). 扬子西缘高温深成的丹巴金矿形成于~185 Ma,晚于区域变质顶峰~193 Ma,其角闪岩相峰期后成矿特征不支持成矿流体来自围岩变质,反之需要外来深源流体(Zhao *et al.*, 2019). 鉴于该区域不存在与成矿同时代俯冲,结合大地构造演化和同位素约束,该成矿流体最可能来自新元古代交代富集的岩石圈地幔脱气(图7c).

4.2.5 证据 相比于中上地壳“变质流体成因模式”和“地幔流体成因模式”得到了更多地质证据的支持. 这些证据包括地表热泉和热液矿床的 He-Ar 和 Re-Os 同位素、地幔起源流体包裹体以及次大陆岩石圈地幔的含金性研究等. 这些证据表明熔体和流体在上地幔共存,并且流体可以通过深大断裂到达上地壳形成金矿床.

(1)地幔中水的存在. 流体包裹体证据主要来自金刚石和地幔起源火山岩中的超基性俘虏体. Schrauder and Navon(1994)在研究 Botswana 的纤维状金刚石中流体包裹体时得到两个组分单元:一个是富碳酸盐和 Ca-Fe-Mg-P-K 氧化物的流体,另一个是富 H₂O、SiO₂ 和 K₂O 的流体. 这项研究首次直接证明在深达下地壳的金刚石稳定区域有流体和熔体共存. Bureau and Keppler(1999)在进行金刚石封闭体高温高压实验时发现,在上地幔环境下花岗岩和玄武岩熔体都可以和含 H₂O 流体完全混溶,因此在上地幔环境不存在水饱和固相线. 尖晶石二辉橄榄岩流体包裹体中富硅熔融包裹体则显示含 H₂O 和硅酸盐成分的超临界流体到达浅部后的不混溶. Bureau and Keppler(1999)推测洋壳板片俯冲时角闪石分解产生高流动性的含 H₂O 流体,而硬柱石和多硅白云母分解更多地产生低流动性富硅酸盐流体. Klein-Ben David *et al.*(2011)的金刚石容器高温高压实验(1 000~1 200 °C; 4~6 GPa)表明,含微小富 Cr 交代矿物(铬铁矿和金云母)包裹体的金刚石会出现在俯冲带和深部岩石圈地幔环境下,富碱含 H₂O 流体则是主要的交代介质.

Andersen and Neumann(2001)在对全球地幔起

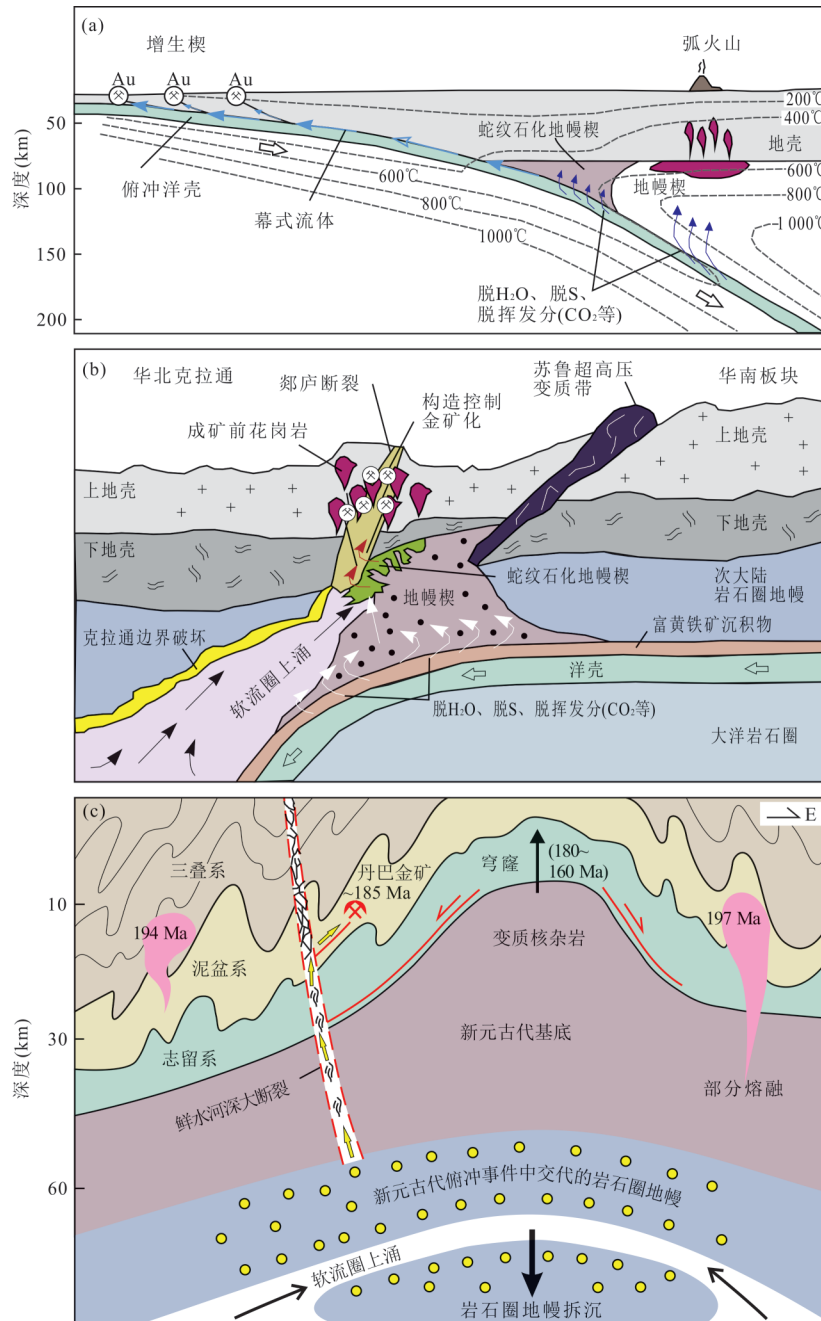


图7 地幔流体成因模式示意

Fig.7 Schematic illustrations of mantle fluid model

a. 俯冲带大洋地壳脱水和回返模式, 据 Peacock(1990) 和 Groves *et al.*(2019); b. 克拉通破坏富集地幔脱气模式, 指示交代岩石圈地幔为流体和金属来源, 据 Goldfarb and Santosh(2014) 和 Deng *et al.*(2015c); c. 岩石圈拆沉富集地幔脱气模式, 指示交代富集岩石圈地幔作为流体储库, 据 Zhao *et al.*(2019)

源俘虏体包裹体研究的综述中指出,地幔起源俘虏体的橄榄石和辉石中含大量富CO₂包裹体、硅酸盐玻璃、固态金属硫化物熔体以及碳酸盐包裹体,表明在上地幔的确存在流体和熔体.Liu and Fei(2006)研究了古亚洲洋蛇绿岩带纯橄榄岩及碰撞后基性—超基性岩,对橄榄石和斜长石的包体进行微激光拉曼测试,结果显示这些岩石带来的地幔流体富H₂O

和CH₄及少量N₂,进一步的氧化还原态、压力和形成深度研究表明,这些流体形成于软流圈,并在洋壳板片的重复俯冲中逐步被H₂O稀释并被氧化.Rospabé *et al.*(2017)在研究Oman蛇绿岩中纯橄榄质壳—幔过渡带的成因时发现,大量含水角闪石和辉石矿物分布在橄榄石和铬铁矿包裹体中,表明这些含水矿物形成时间早而且温度高,并认为过渡带

中洋中脊玄武岩质熔体受到了超临界硅饱和流体的混染.基于这类岩石学和岩相学证据,Rospabé *et al.*(2017)认为Oman壳—幔过渡带下存在热液成因的水.

(2)地幔流体浅表显示.Kennedy(1997)在研究美国西海岸San Andreas断层系统时就发现,断层上热泉的 $^3\text{He}/^4\text{He}$ 比值很高,且与围岩地质及其流体特征没有关联,因此认为热泉起源于通过韧性下地壳来自地幔的流体.Kennedy and van Soest(2007)和Piliét *et al.*(2011)针对San Andreas断层的放射性同位素、卤素及惰性气体研究也得出了相同的结论.Kl-emperer *et al.*(2013)在研究西喜马拉雅Karakoram岩石圈规模走滑断层上的热泉时,根据其超过地壳值100倍的 $^3\text{He}/^4\text{He}$ 值认为,部分热液系统成分一定起源于构造活跃的地幔.甚至在研究普遍认为成矿空间和时间上均与地壳重熔(S型花岗岩)密切相关的钨锡矿床时,Burnard and Polya(2004)也认为葡萄牙Panasqueira矿床毒砂和黑钨矿 $^3\text{He}/^4\text{He}>5\text{Ra}$ 的比值只能解释为地幔成因,而且与花岗岩无关.

Re-Os同位素证据则来自油田地球化学.Finlay *et al.*(2010)在研究英国北海石油成因时发现,大型盆地边界断层上的石油 $^{187}\text{Os}/^{188}\text{Os}$ 值不具放射性(非地壳成因),而远离断层的 $^{187}\text{Os}/^{188}\text{Os}$ 值则具有放射性(地壳成因).因此,Finlay *et al.*(2010)认为北海盆地边界断层已渗透到Moho边界,为幔源流体提供通道进入北海油田.

(3)大陆岩石圈地幔含金性.软流圈地幔通常含有 1×10^{-9} 的金含量,交代的大陆岩石圈地幔金含量为 14×10^{-9} ,地幔捕虏体内黄铁矿中金含量高达 5×10^{-6} (Griffin *et al.*, 2013).因此这种次大陆岩石圈地幔可以作为产于克拉通边缘的造山型金矿的流体和金属来源(Groves and Santosh, 2015),尤其是产于角闪岩相的金矿床,例如扬子西缘丹巴金矿(Zhao *et al.*, 2019).Hronsky *et al.*(2012)将交代富集岩石圈地幔推广为增生造山带内造山型金矿统一的物质来源.

4.2.6 适用性 地幔流体成因模式可以解释造山型金矿中具有普适性的现象:(1)成矿时代.形成时代上成矿和变质事件与岩浆活动可以不一致,因为成矿流体与区域变质和岩浆活动是伴生关系,而无成因联系;(2)成矿深度.由于成矿流体来自深部,造山型金矿可以形成在次绿片岩相到麻粒岩相深度范围内;(3)物质来源.大部分造山型金矿床的稳定同位

素和放射性同位素呈现出混合特征,反映了深源流体经历过广泛的地壳深度范围.地幔流体模式不需要地壳中的变质火山岩/变质沉积岩作为源岩,其最终源岩是俯冲洋壳板片和上覆富Au黄铁矿沉积物.交代富集地幔在后来造山事件中作为许多类型矿床的成矿物质来源已被许多学者认识到(Bierlein and Pisarevsky, 2008; De Boorder, 2012; Hronsky *et al.*, 2012; Webber *et al.*, 2013).因此, Groves *et al.*(2019)认为地幔流体模式可以作为造山型金矿统一的成因模式.

地幔流体模式的瓶颈在于深部机制.上述富 $\text{H}_2\text{O}-\text{CO}_2-\text{CH}_4$ 的地幔流体证据表明,上地幔或交代地幔的确存在含水流体,并在地表热泉和矿床中有所显示.但这类超临界流体如何通过下地壳,特别是交代富集地幔释放的流体进入下地壳而不引起部分熔融? Zhao *et al.*(2019)解释为超临界流体根据水力压裂的方式通过岩石圈规模的深大断裂形成造山型金矿(地震泵吸; Cox, 2016),如果流体快速通过水饱和的深大断裂,且流体通道是开放体系而非封闭体系,则可能避免引起部分熔融(Seno and Kirby, 2014).尽管有这类解释,但要论证该机制需要更多涉及壳幔作用的实验岩石学等工作;这类工作研究程度往往很低,制约了我们对地幔含金流体的理解(Groves *et al.*, 1998; Groves and Santosh, 2016).

4.3 岩浆热液成因模式

岩浆热液流体作为造山型金矿物质来源存在较大争议,争议的焦点为造山型金矿与岩浆活动的时间、空间、元素组合的关系.例如, Wall *et al.*(2004)认为世界最大的造山型金矿Muruntau成矿流体来自矿区深部3~4 km花岗岩,其证据为Muruntau金矿形成时间与岩体侵位时间一致,以及矿体具有异常的As、Bi、K、Mo、S、Sb、W元素含量.然而Goldfarb and Groves(2015)认为这些元素异常并不能指示来自岩浆熔体出溶,其同样可以来自围岩(碳质泥岩).在中国胶东金成矿带,由于矿体与侏罗纪、白垩纪花岗岩、煌斑岩和辉绿岩脉具有紧密的空间联系,岩浆热液流体已经成为其潜在的流体来源(Hart, 2005).然而成矿与岩浆活动缺少时间关联、缺少有意义的金属纵向分带、矿体受区域断裂系统控制等特征与上地壳岩浆流体出溶导致的成矿特征不一致(Goldfarb and Groves, 2015).也有学者认为造山型金矿与煌斑岩体有成因上的联系,而Wyman(1989)发现太古代钾玄质岩浆具有低的金含量、煌

斑岩与金矿化并非同期,煌斑岩物源来自俯冲带岩浆作用而并非富金地幔,大部分煌斑岩出现在缺少造山型金矿的大陆裂谷和大洋岛弧环境,这些证据并不支持煌斑岩岩浆作为流体和物质来源.这个观点得到 Müller and Groves (1997)研究结论的支持.

Bath *et al.* (2013)在研究 Yilgarn 克拉通 East Repulse 矿床时发现从矿化带远端或下盘到内侧黑云母和磷灰石中 K 和 F 元素含量逐渐降低,这种现象与岩浆热液出溶导致的陡元素梯度一致.但是矿化带下盘石膏、重晶石等矿物指示氧化环境,因此与从矿脉外侧运移并氧化的还原流体相矛盾 (Evans *et al.*, 2006; Evans, 2010). 尽管一些研究仍然认为造山型金矿存在岩浆热液流体贡献,例如 Abitibi 带 Malartic 金矿 (Groves *et al.*, 2003)、苏格兰 Cononish 金矿 (Spence-Jones *et al.*, 2018)、西非马里 Loulo 金矿 (Lawrence *et al.*, 2013) 等,但是由于缺少新的有力的证据证明造山型金矿成矿流体来自岩浆热液, Goldfarb and Groves (2015) 认为岩浆热液流体并不是造山型金矿的流体和物质来源. 我们同意这一观点,因为造山型金矿与 Sillitoe (1991) 提出的侵入体相关金矿具有诸多相似特征 (Sillitoe and Thompson, 1998). 如果造山型金矿物源来自岩浆热液流体,那么区分这两种类型金矿将毫无意义 (Sillitoe, 2008), 因此我们认为岩浆热液流体来源的造山型金矿应该归类为侵入体相关金矿.

5 中国造山型金矿

随着华北板块和华南板块依次向古欧亚板块的拼合,各造山带及相应的成矿带的形成时代呈有规律的分布. 中国造山型金可划分为江南造山带志留纪成矿带 (王学明等, 2000; Zhu and Peng, 2015)、阿尔泰—天山二叠纪成矿带 (Zhang, L. C. *et al.*, 2003; Zhang, L. *et al.*, 2012)、华北克拉通北缘三叠—侏罗纪成矿带 (毛景文等, 2005; 陈衍景等, 2009; Deng *et al.*, 2009b, 2014c; Li *et al.*, 2012a, 2012b; Song *et al.*, 2016; Jia *et al.*, 2018)、特提斯造山带二叠—侏罗纪成矿带 (Deng *et al.*, 2010a, 2014a, 2014b; Ding *et al.*, 2014; Liu *et al.*, 2015a)、华南板块晚三叠世—侏罗纪成矿带 (毛景文等, 2004; Chen *et al.*, 2011)、华北克拉通东南缘白垩纪成矿带 (Mao *et al.*, 2002, 2008, 2011; 陈衍景等, 2004; Chen *et al.*, 2008)、青藏高原及周缘古近纪成矿带 (Hou *et al.*, 2007; Li *et al.*, 2007; Hou and Cook, 2009; Jiang

et al., 2009; 邓军等, 2011; Sun *et al.*, 2014) 等七大成矿带 (图 8). 各成矿带分布主要受到了显生宙不同时代造山作用的控制, 赋存于造山带内部, 大部分成矿带受到了复合造山作用的强烈影响. 下文主要介绍近年来新近发现和成因争议较大的三大成矿带.

5.1 特提斯二叠—侏罗纪成矿带

特提斯二叠—侏罗纪造山型金矿成矿带主要分布于祁连山—昆仑山造山带和松潘—甘孜褶皱带. 该带东缘分布有新元古代岩浆弧带 (Zhou *et al.*, 2002a, 2008) 和 > 1 000 km 的中生代穹隆带 (Zhao *et al.*, 2019); 其北部和西部分别为晚二叠古特提斯洋闭合形成的阿尼玛卿缝合带和甘孜—理塘缝合带 (Deng *et al.*, 2014a). 自中生代以来, 该带经历三大构造演化: ①晚三叠世俯冲挤压, 其间地壳缩短致使松潘—甘孜褶皱带的形成, 发育强烈褶皱、逆冲推覆和巴罗式高温变质作用; ②早侏罗沿龙门山形成的穹隆伸展作用; ③印度—欧亚板块碰撞引起的新生代逆冲推覆. 区域上岩浆岩主要为晚三叠—早侏罗后碰撞和碰撞后花岗岩, 主要包括 220~200 Ma I 型、埃达克质岩和 200~180 Ma A 型、S 型花岗岩 (Zhang *et al.*, 2007).

该成矿带包括的典型矿床有五龙沟、大厂和丹巴等金矿. 下文以丹巴金矿为例介绍该成矿带特征. 丹巴金矿产在变质核杂岩边部泥盆系角闪岩相沉积变质岩中 (Weller *et al.*, 2013), 围岩顶峰变质在 ~193 Ma, 温度压力在 6 ± 0.5 kbar 和 650 ± 50 °C; 退变质在 ~188 Ma, 温度压力在 4.5 ± 0.5 kbar 和 550 ± 50 °C (Zhao *et al.*, 2019). 矿床赋存于近顺层发育的脆韧性剪切带中, 蚀变以高温而窄的黑云母蚀变带和角闪石—斜长石—钾长石蚀变矿物为特征. 矿石矿物早期以磁黄铁矿为主, 晚期以与自然金共生的叶碲铋矿为主. 成矿流体为低盐度 (~2% Na-Cleqv)H₂O-CO₂-CH₄ 流体. 辉钼矿 Re-Os 定年、蚀变矿物温压计算和包裹体测温表明成矿发生在 185 ± 9 Ma, 温度压力在 4~5 kbar 和 500~650 °C (Zhao *et al.*, 2019). 综合表明丹巴金矿为早侏罗高温深成造山型金矿, 成矿于区域变质峰期之后的退变质阶段. 矿床的初始高温压条件, 结合其确定的晚变质成矿时限, 使得成矿流体不太可能来自围岩沉积岩系的液化, 反之需要的是一个来自深部的外来成矿流体. 基于该区域的大地构造演化史, 结合地质和同位素证据, 最可能的来源是新元古代俯冲相关的交代岩石圈地幔 (Zhou *et al.*, 2002a, 2008). 在早侏罗碰撞后

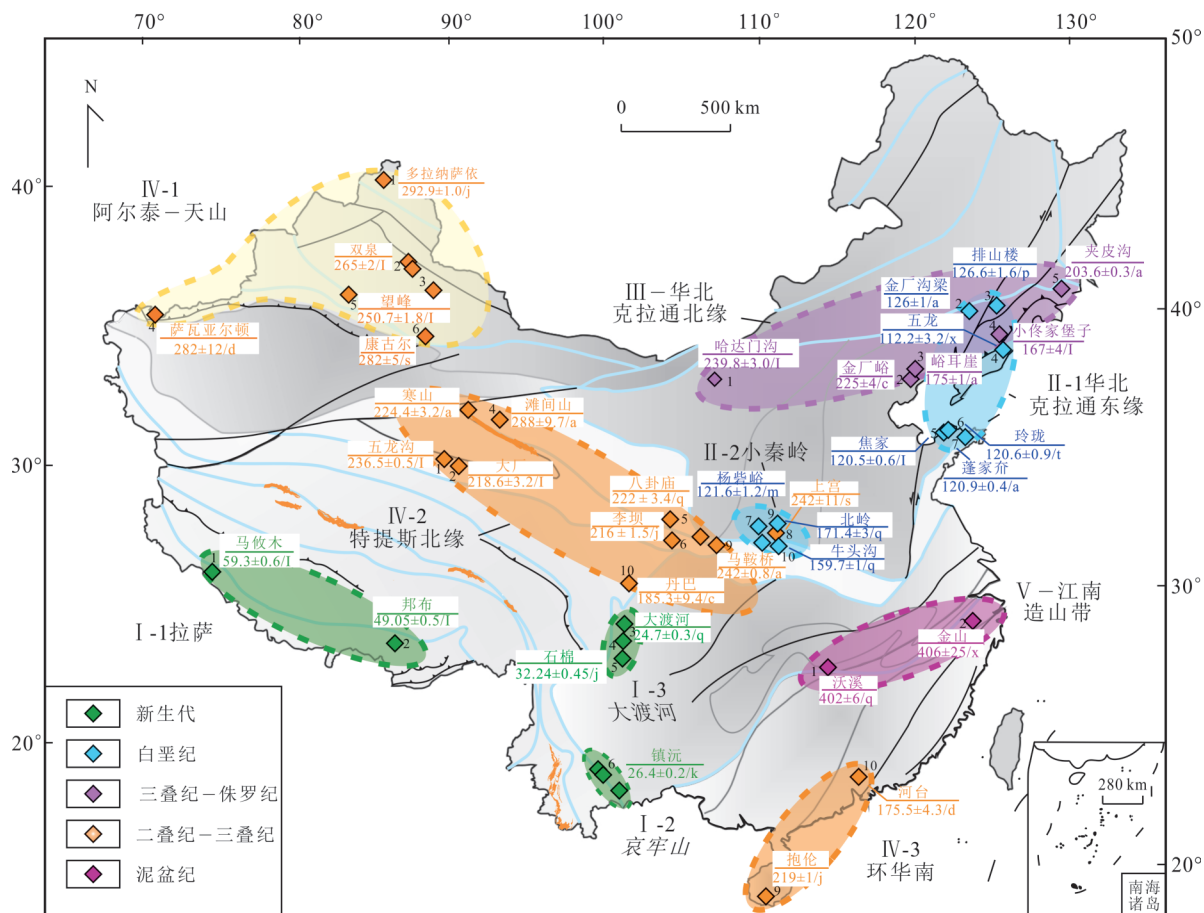


图 8 中国造山型金矿成矿带划分

Fig.8 Chinese orogenic gold belts divided by orogens and their forming ages

据 Deng and Wang(2016);典型造山型金矿带分布:a.Zr/U-Pb;b.Mol/Re-Os;c.Py/Re-Os;d.Apy, Re-Os;e.Ser/Ar-Ar;f.Ms/Ar-Ar;g.Phl/Ar-Ar;h.Bt/Ar-Ar;i.Kfs/Ar-Ar; j.scheelite/Sm-Nd;k.Ser/Rb-Sr

伸展环境中,软流圈上涌加热再活化 K-H₂O-CO₂ 交代和成矿金属富集了的岩石圈地幔,使其释放含金 H₂O-CO₂-CH₄ 成矿流体.这个深源的高温超压成矿流体通过鲜水河深大断裂向上输运后就位于穹隆边部脆韧性剪切带中.

丹巴金矿是全球第三例详细报道有着规模储量产在角闪岩相带内的显生宙高温造山型金矿.它与世界范围内产在太古代绿岩带内的大部分高温金矿床以及法国 Massif Central 金矿田的显生宙高温金矿相似(Bouchot *et al.*, 2005).法国 Massif Central 地区早期为俯冲与挤压造山;晚期为碰撞后转换挤压到穹隆伸展背景下的金成矿.二者时代相差达 200 Ma,与金矿化相关的穹隆带与造山带往往平行(Whitney *et al.*, 2004).

5.2 华北克拉通东南缘白垩纪成矿带

华北克拉通东南缘是中国最大的金产地,包括胶东和秦岭地区.华北克拉通东缘和南缘分别分布

着一系列变质核杂岩,空间上与形成于早白垩纪的裂谷盆地耦合(Davis *et al.*, 2002).因此,众多学者认为华北克拉通大规模岩石圈减薄或破坏发生在白垩纪(Yang *et al.*, 2003; Li *et al.*, 2012a; Yang and Santosh, 2015);减薄后的岩石圈厚度在 60~120 km,具有高热流值.胶东成矿带范围由北-北东向的郯庐断裂和苏鲁超高压变质带限定(Deng *et al.*, 2009a, 2010b, 2011).胶东地区的基底主要由新太古代和稍年轻的胶东群 TTG(英云闪长岩-奥长花岗岩-花岗闪长岩)片麻岩,以及元古代粉子山群和新元古代蓬莱组群变质沉积岩组成(Tang *et al.*, 2007).区域花岗岩类形成时限大致在 225~205 Ma、160~150 Ma、130~120 Ma 和 ~90 Ma(Chen *et al.*, 2008).

胶东大部分的金矿受北东向和北北东向脆-韧性断裂控制,穿切玲珑和郭家岭等岩体,切穿基底岩石(Yang *et al.*, 2016a, 2016b, 2016c).这些北东

向断层大致平行展布,间距大约为 35 km.从西到东分别是三山岛、焦家、招一平、栖霞、牟平—即墨和牟乳断裂,它们控制了胶东成矿带 90% 金的产出.这些控矿的北东向断裂成矿后仍然活动(Yang *et al.*, 2013).金矿化有两种形式:一种是石英脉(玲珑式),沿走滑断层延伸超过 1 km;另一种是破碎蚀变岩型(焦家式),分布在胶东北西部(Yang *et al.*, 2009a, 2016a; Deng *et al.*, 2011).矿化的空间分布部分受控于蚀变和矿化过程中的水—岩反应(Yang *et al.*, 2015).沿着胶莱盆地北缘,有几处金矿床产出于角砾状古元古代变质岩或白垩纪沉积岩中,其中以蓬家夬金矿(蓬家夬式)为典型代表(Li *et al.*, 2006).矿石中绢云母 $^{40}\text{Ar}/^{39}\text{Ar}$ 定年表明胶东金矿床主要成矿于 120 ± 10 Ma, 同期发育活化正断层(Deng *et al.*, 2015a).

胶东代表型矿床包括大尹格庄、新城和蓬家夬等矿床.大尹格庄金矿位于招一平断裂中段(Deng *et al.*, 2011),断层上盘为胶东群变质岩,下盘为玲珑花岗岩.上盘岩石发育碳酸盐化、绿泥石化、弱硅化和金矿化,金品位低于 0.1 g/t.金矿化主要产于下盘,并稳定往下延伸(Wang *et al.*, 2010a, 2010b).矿体主要发育在黄铁矿化、绢英岩化和有不同破裂程度硅化的花岗岩中(Deng *et al.*, 2009a),张性剪切带发育厚大矿体.新城金矿产于玲珑黑云母花岗岩和郭家岭花岗闪长岩中(Wang *et al.*, 2015a),包含“焦家式”和“玲珑式”矿化类型.浸染网脉状“焦家式”矿石产于焦家断层破碎带,而次要的雁列状张性“玲珑式”含金脉赋存在北东—北北东向切穿花岗岩的次级断裂中.矿体周围发育强烈绢云母化、硅化和钾化.

5.3 青藏高原及周缘古近纪成矿带

青藏高原是全球规模最宏大、特征最典型、时代最年轻的大陆碰撞造山带,也是世界三大巨型成矿域之一——特提斯成矿域的重要组成部分.除发育超大型斑岩型 Cu 矿、类 MVT 型 Pb-Zn 矿和造山型 Au 矿等重要金属矿床外,也是碰撞造山型金矿的重要成矿区(Deng and Wang, 2016; Sun *et al.*, 2016; 李华健等, 2017).青藏高原碰撞过程形成了系列造山型金矿,可归纳为与大规模地壳挤压、剪切和旋转有关的三套造山型金成矿系统,其成矿作用与区域大型岩石圈不同性质的构造体制转换密切相关.相对于其他构造背景下的成矿作用,其和大陆碰撞有关的金成矿作用呈现了成矿周期多、矿化

样式复杂和成矿环境多样的特征.

与大型挤压有关的成矿系统形成于 50~40 Ma,沿雅鲁藏布江缝合带分布.雅鲁藏布江缝合带位于南拉萨地块与喜马拉雅地块之间,东西向延伸 2 500 km,被广泛认为是欧亚板块和印度板块的交界(Harrison *et al.*, 2000; Dai *et al.*, 2012; Wang *et al.*, 2015b).雅鲁藏布江缝合带由北向南主要包含三个构造单元:日喀则弧前盆地、蛇绿岩带及三叠纪—始新世增生楔(王学明等, 2000; Malpas *et al.*, 2003; Li *et al.*, 2009).造山型金矿形成于大陆主碰撞和峰期变质背景,成矿年龄集中在 44~59 Ma(Jiang *et al.*, 2009; Sun *et al.*, 2016; 李华健等, 2017),由西至东依次包含有马攸木($^{40}\text{Ar}/^{39}\text{Ar}$: 59.3 ± 0.62 Ma; Jiang *et al.*, 2009)、邦布($^{40}\text{Ar}/^{39}\text{Ar}$: 44.8 ± 1.0 Ma; Sun *et al.*, 2016)、折木郎及念扎金矿($^{40}\text{Ar}/^{39}\text{Ar}$: 43.66 Ma)等;矿床主要受控于近 EW 向脆韧性剪切带的次级张性构造(Sun *et al.*, 2016).

大型剪切有关的成矿系统主要形成于青藏高原东南缘的哀牢山造山带.哀牢山造山带主要经历新元古代大洋俯冲(~840 Ma)、三叠纪古特提斯洋闭合及新生代大型剪切(32~25 Ma; Gao *et al.*, 2018; Wang *et al.*, in review).哀牢山剪切带主要为东部高级变质中的韧性剪切带以及西部低级变质中的脆性剪切带(Lin *et al.*, 2012; Liu *et al.*, 2015b).造山型金矿均分布在由西部的古生代—三叠纪地层构成的低级变质带上,其中大型金矿由北向南包含有镇沅、金厂、墨江及长安金矿(Li *et al.*, 2019a, 2019b).矿床主要赋存在发育志留纪至二叠纪沉积岩组成的紧闭褶皱中,上三叠统红色砂页岩宽缓褶皱作为盖层;S-He-Ar-C-O 同位素表明地幔流体为成矿的重要来源(Sun *et al.*, 2009; 梁业恒等, 2011);和大型剪切有关的成矿作用同期的地质事件包括变沉积岩、变火山岩等岩石变质(产生了不同类型淡色花岗岩和石英脉)以及区域的伸展和抬升(Cao *et al.*, 2011).

中新世时期后碰撞伸展环境,喜马拉雅造山带东部形成一系列金锑矿床,由西向东包含沙拉岗(U-Pb: 晚于 23.6 Ma; 张刚阳等, 2011)、马扎拉及查拉普等.矿床均分布在藏南拆离断层系(STDS)相关的构造热液穹隆中(Yang *et al.*, 2009b),穹隆被中新世淡色花岗岩侵入.矿床受控于 E-W 走向的拆离断层和 N-S 走向的正断层以及它们的交汇处,热液穹隆和张性构造是 Sb-Au 矿床形成的重要因素.成矿金属

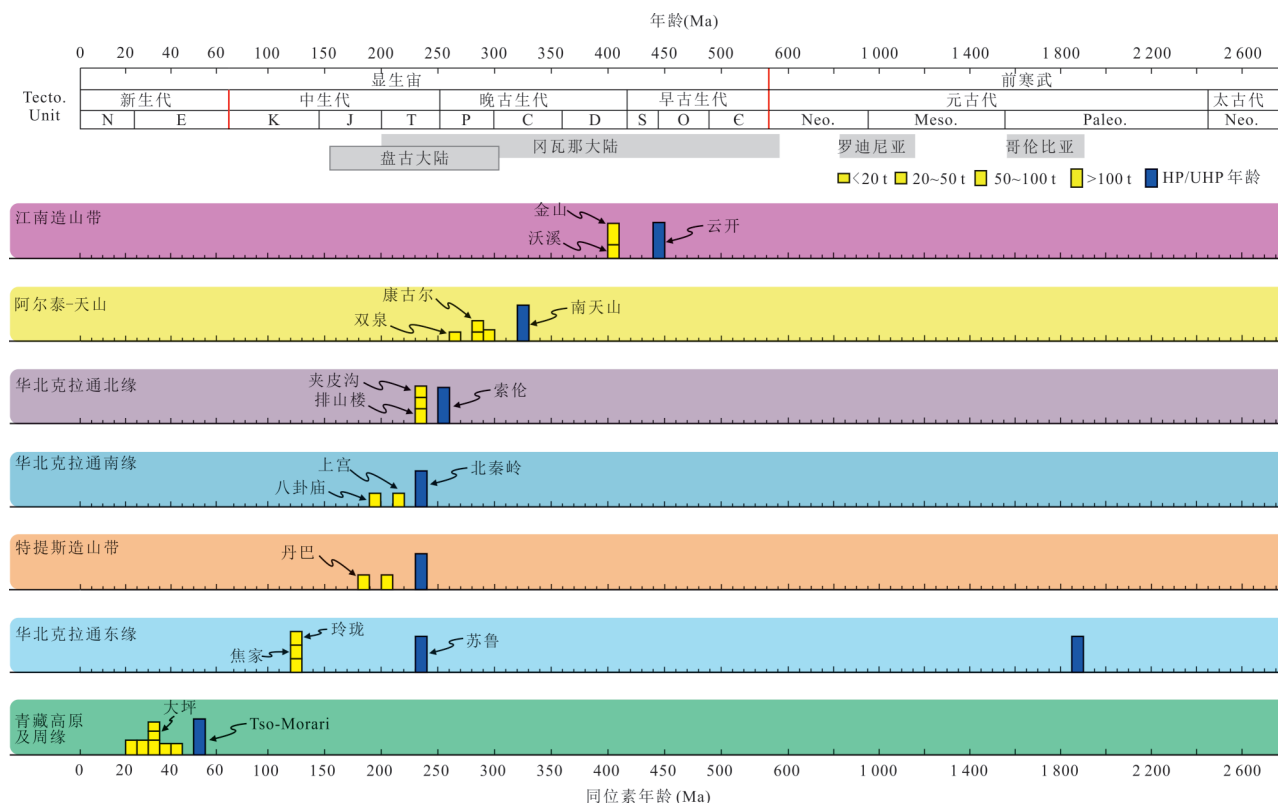


图9 中国造山型金成矿与超高压变质时代对比

Fig.9 Age contrasts between Chinese orogenic gold deposits and ultra-high pressure metamorphism
据 Deng and Wang(2016)

认为主要来源于围岩(Zhai *et al.*, 2014). 区域同期的构造热事件包括NS向高角度断层及裂谷以及大型拆离断层(Williams *et al.*, 2001, 2004)、EW走向淡色花岗岩脉的形成(Guo *et al.*, 2013)以及高Sr/Y特征的花岗类斑岩的侵入(Hou and Cook, 2009; Hou *et al.*, 2015; Wang *et al.*, 2015b).

5.4 成因模式

从成矿时代上来说,各成矿带金矿往往形成于区域超高压变质之后(图9). 例如~400 Ma江南造山带金矿带形成于~450 Ma云开超高压变质之后(王学明等, 2000; Wang *et al.*, 2013); 300~280 Ma天山-阿尔泰成矿带形成于~330 Ma南天山超高压变质之后(Du *et al.*, 2014); 240~180 Ma华北克拉通北缘成矿带形成于~260 Ma索伦超高压变质之后(Jia *et al.*, 2018); 200~180 Ma特提斯成矿带形成于~240 Ma超高压变质之后(Liu *et al.*, 2015a)、160~120 Ma华北克拉通东南缘成矿带形成于~240 Ma北秦岭和苏鲁超高压变质之后(Li *et al.* 2008); 50~20 Ma青藏高原及周缘成矿带形成于~50 Ma Tso-Morari超高压变质之后(Jiang *et al.*, 2009). 各大成矿带主体形成于造山作用峰期变质之后,因此需要外

来深成的流体来源.

以具体矿床为例,长安金矿矿化岩石的古地磁数据表明金矿化晚于剪切活动结束时限(~21 Ma), 此时哀牢山带发育退变质作用,因此用变质流体成因模式无法解释哀牢山带成矿作用(Gao *et al.*, 2018). 古地磁学研究表明镇沅和长安金矿古纬度分别为 $19.9^{\circ} \pm 3.6^{\circ}N$ 和 $16.2^{\circ} \pm 2.9^{\circ}N$. 这两处金矿的古纬度与从景谷中新统地层得到的结果基本一致 ($19.0^{\circ} \pm 3.6^{\circ}N$),但完全不同于白垩纪一始新世古地磁数据显示比较统一的较高的古纬度 ($28.4^{\circ} \pm 1.1^{\circ}N$),说明这两个金矿形成于红河-哀牢山剪切带大规模走滑后(图10; Gao *et al.*, 2018). Wang *et al.* (in review)基于以上证据提出,在区域大规模走滑末期的伸展-变质背景下,富集岩石圈地幔上涌,释放幔源流体,沿区域尺度剪切带上移到次级剪切带-断裂带、岩性接触带等构造有利部位,并与不同围岩发生水岩反应淋滤围岩成矿物质,硫氰酸根中硫与富铁岩石(如大坪闪长岩、镇沅金矿和墨江-金厂基性超基性岩、煌斑岩)反应形成黄铁矿、毒砂等矿物,引起含金络合物失稳和金等成矿元素沉淀.

丹巴金矿成矿流体为低盐度(~2 % NaCl_{eqv})

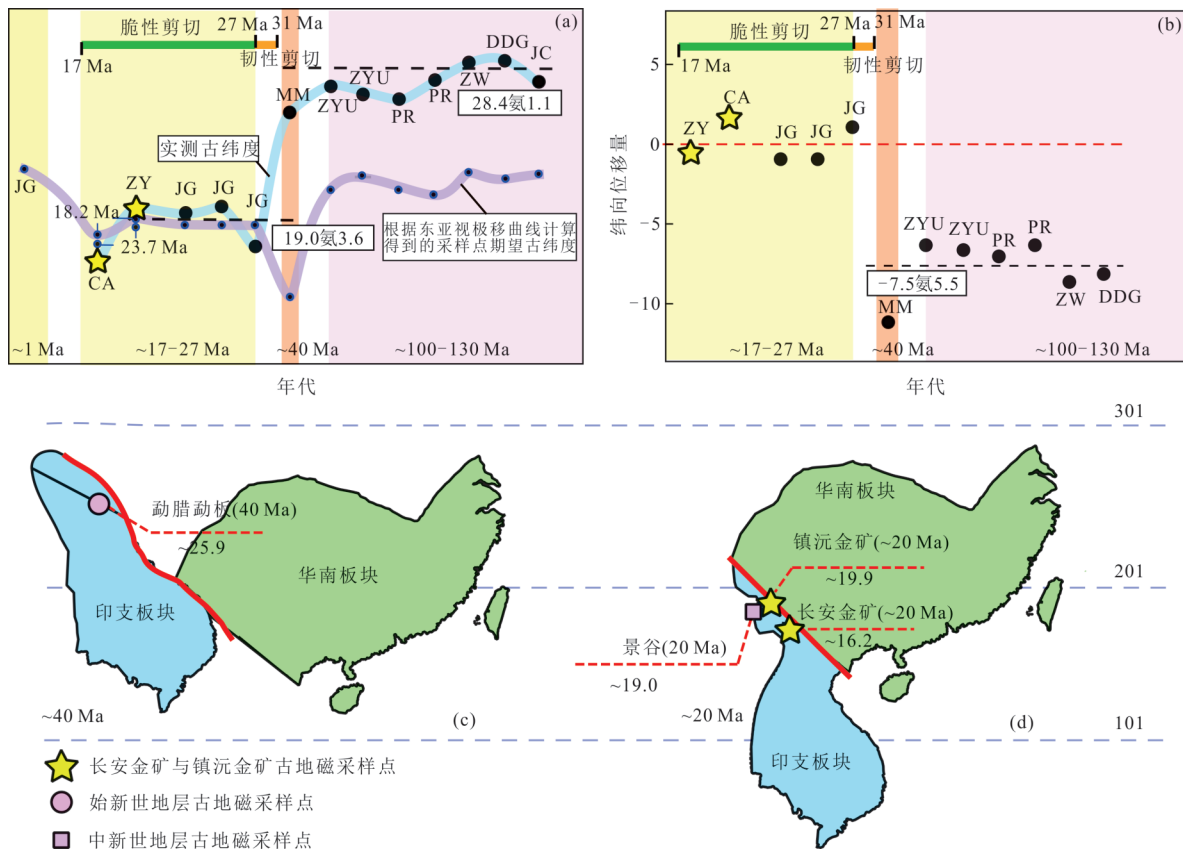


图 10 矿床古地磁研究限定成矿与剪切时代

Fig.10 Deposit paleomagnetism data constrain mineralization and shearing ages

据 Gao *et al.* (2018); a. 印支地块不同地区 130~20 Ma 期间的古纬度值: $28.4^{\circ} \pm 1.1^{\circ}$ N 与 $19.0^{\circ} \pm 3.6^{\circ}$ N 分别代表印支地块 130~40 Ma 和 20 Ma 的平均古纬度值; b. 印支地块不同地区相对于东亚稳定区的纬向滑移量: $-7.5^{\circ} \pm 5.5^{\circ}$ 为印支地块自 40 Ma 到 20 Ma 期间的平均南向滑移量; c、d. 印支地块相对于华南板块在 40 Ma 和 20 Ma 的古地理位置

$H_2O-CO_2-CH_4$ 流体, 成矿发生在 4~5 kbar、500~650 °C, 属于高温深成矿床 (Zhao *et al.*, 2019). 胶东金矿床的流体包裹体特征基本相同 (Fan *et al.*, 2003; Deng *et al.*, 2015c; Li *et al.*, 2015; Yang *et al.*, 2016a), 包括三种类型原生包裹体: 富水含 CO_2 液相、富 CO_2 液相和少量 CO_2 包裹体. 流体成分为 6%~10% CO_2 、3.6%~4.5% NaCl_{eq} 和 0.5% CH_4 , 捕获温度压力在 ~236~336 °C 和 ~1.7 kbar (Yang *et al.*, 2016a). 哀牢山造山型金矿流体包裹体研究表明成矿流体为低盐度 (~1.8%~14.8%)、中低温 (~150~350 °C)、富集 CO_2 的 NaCl-H₂O 流体系统. 大坪金矿成矿流体温度在 270~300 °C, 成矿深度预测为 5~13 km (毕献武等, 1997; Zhu *et al.*, 2011); 三处浸染型金矿成矿流体温度在 240~180 °C, 成矿深度预测为 1~3 km (梁业恒等, 2011; 李士辉等, 2011), 可能为浅成造山型金矿.

丹巴金矿磁黄铁矿中流体包裹体 $^3He/^4He$ 比值

在 0.1~0.5 R/Ra, $^{40}Ar/^{36}Ar$ 比值为 300~600; 胶东金矿带黄铁矿中流体包裹体 $^3He/^4He$ 比值为: 蓬家乔金矿 0.38~0.79 R/Ra, 邓格庄 1.93~2.14 R/Ra, 焦家 1.64~2.36 R/Ra; $^{40}Ar/^{36}Ar$ 比值显示蓬家乔为 310~393、邓格庄为 680~756、焦家为 500~1148 (Zhang *et al.*, 2008). 基于胶东的数据, Zhang *et al.* (2008) 解释这些金矿的流体来源混入了幔源成分. 哀牢山金矿带碳酸盐 C-O 和黄铁矿 He-Ar 同位素测试同样支持一个壳幔共同参与的流体来源. 鉴于哀牢山金矿带成矿晚于区域变质, 这个源区很可能是地幔 (Wang *et al.*, in review). 围岩蚀变、含金黄铁矿微量组成以及高度分散的硫同位素组成指示了一个外来深成流体来源, 成矿流体上升途中遭受了改造 (Wang *et al.*, in review). 综上所述, 丹巴、胶东和哀牢山等重要金矿和矿集区的物质来源倾向于地幔流体成因模式.

6 结论

(1)造山型金矿是产在次绿片岩相到麻粒岩相变质岩中的一组连续的同成因矿床组合,主要沿活动大陆边缘带分布,产于挤压到伸展的转换背景.增生楔、弧前和弧后倒转盆地伸展环境下软流圈上涌引起的高温低压变质是区域尺度金成矿的深部驱动机制.全球造山型金矿主要形成于超大陆拼合陆壳增生峰期: >3.0 Ga、 $2.8\sim 2.55$ Ga、 $2.1\sim 1.8$ Ga和 <0.57 Ga.

(2)造山型金矿成矿流体迁移中 Au 主要以 $\text{Au}(\text{HS})_2^-$ 络合物形式存在; CO_2 以 H_2CO_3 形式维持流体 pH 值平衡,进而保持 Au 溶解度.构造控矿形式包括:褶皱转折端和层间滑脱带、剪切带张性或压性衔接部位、断裂弯曲转折端和里德尔剪切派生裂隙等.水岩反应导致金沉淀是造山型金成矿主要机制之一.

(3)随着大量新的地质年代学和地球化学研究,大气降水和岩浆—热液流体作为造山型金矿主要流体来源已被排除.于是关于造山型金矿的成因讨论集中在两种模式上:中上大陆地壳绿片岩相—角闪岩相进变质流体成因、幔源流体(俯冲洋壳脱水或交代岩石圈地幔液化)成因.变质流体成因模式适用于全球众多产在绿片岩相中显生宙造山型金矿;地幔流体模式则可以解释许多特殊的矿床,比如全球前寒武纪深成造山型金矿和中国许多显生宙造山型金矿.

(4)中国造山型金矿可分为江南造山带志留纪成矿带、天山—阿尔泰二叠纪成矿带、华北克拉通北缘三叠—侏罗纪成矿带、特提斯造山带二叠—侏罗纪成矿带、华南板块晚三叠世—侏罗纪成矿带、华北克拉通东南缘白垩纪成矿带、青藏高原及周缘古近纪成矿带等七大成矿带,以显生宙成矿为其特点,主体形成于区域变质峰期之后.胶东、哀牢山、丹巴等金矿(带)的研究都支持了幔源流体参与成矿的观点.

造山型金矿后续研究方向包括:(1)精确厘定成矿时代,查明成矿与围岩变质、岩浆活动和构造变形的关系,揭示区域构造演化对造山型金成矿控制;(2)建立更全面和可靠研究方式来反演示踪,探讨地幔流体富集、储存和释放的主要机制;(3)阐释岩石圈多尺度构造控矿网络,研究成矿流体输运过程和控制机理等.

References

Andersen, T., Neumann, E.R., 2001. Fluid Inclusions in Mantle Xenoliths. *Lithos*, 55(1): 301–320. <https://doi.org/>

10.1016/s0024-4937(00)00049-9

Barley, M.E., Groves, D.I., 1992. Supercontinent Cycles and the Distribution of Metal Deposits through Time. *Geology*, 20(4):291–294.

Bath, A.B., Walshe, J.L., Cloutier, J., et al., 2013. Biotite and Apatite as Tools for Tracking Pathways of Oxidized Fluids in the Archean East Repulse Gold Deposit, Australia. *Economic Geology*, 108(4): 667–690. <https://doi.org/10.2113/econgeo.108.4.667>

Bell, R.M., Kolb, J., Waight, T.E., 2018. Assessment of Lithological, Geochemical and Structural Controls on Gold Distribution in the Nalunaq Gold Deposit, South Greenland Using Three-Dimensional Implicit Modelling. *Geological Society, London, Special Publications*, 453(1): 385–405. <https://doi.org/10.1144/sp453.2>

Bi, X.W., Hu, R.Z., He, M.Y., 1997. Characteristics of Ore-Forming Fluid of Three Gold Deposits in Ailaoshan Gold Mineralization Belt. *Acta Mineralogica Sinica*, 17(4):435–441 (in Chinese with English abstract).

Bierlein, F.P., Crowe, D.E., 2000. Phanerozoic Orogenic Lode Gold Deposits. *Reviews in Economic Geology*, 13: 103–139.

Bierlein, F.P., Groves, D.I., Goldfarb, R.J., et al., 2006. Lithospheric Controls on the Formation of Provinces Hosting Giant Orogenic Gold Deposits. *Mineralium Deposita*, 40(8): 874–886. <https://doi.org/10.1007/s00126-005-0046-2>

Bierlein, F.P., Maher, S., 2001. Orogenic Disseminated Gold in Phanerozoic Fold Belts: Examples from Victoria, Australia and Elsewhere. *Ore Geology Reviews*, 18(1–2): 113–148. [https://doi.org/10.1016/s0169-1368\(01\)00019-1](https://doi.org/10.1016/s0169-1368(01)00019-1)

Bierlein, F.P., Pisarevsky, S., 2008. Plume-Related Oceanic Plateaus as a Potential Source of Gold Mineralization. *Economic Geology*, 103(2): 425–430. <https://doi.org/10.2113/gsecongeo.103.2.425>

Blenkinsop, T.G., Doyle, M.G., 2014. Structural Controls on Gold Mineralization on the Margin of the Yilgarn Craton, Albany - Fraser Orogen: The Tropicana Deposit, Western Australia. *Journal of Structural Geology*, 67: 189–204. <https://doi.org/10.1016/j.jsg.2014.01.013>

Bouchot, V., Ledru, P., Lerouge, C., et al., 2005. Late Variscan Mineralizing Systems Related to Orogenic Processes: The French Massif Central. *Ore Geology Reviews*, 27(1–4): 169–197. <https://doi.org/10.1016/j.oregeorev.2005.07.017>

Breeding, C.M., Ague, J.J., 2002. Slab-Derived Fluids and Quartz-Vein Formation in an Accretionary Prism, Otago

- Schist, New Zealand. *Geology*, 30(6):499–502.
- Browning, P., Groves, D.I., Blockley, J.G., et al., 1987. Lead Isotope Constraints on the Age and Source of Gold Mineralization in the Archean Yilgarn Block, Western Australia. *Economic Geology*, 82(4): 971–986. <https://doi.org/10.2113/gsecongeo.82.4.971>
- Bucher, K., Grapes, R., 2011. *Metamorphism of Pelitic Rocks (Metapelites). Petrogenesis of Metamorphic Rocks.* Springer, Heidelberg, Berlin, 257–313.
- Bureau, H., Keppler, H., 1999. Complete Miscibility between Silicate Melts and Hydrous Fluids in the Upper Mantle: Experimental Evidence and Geochemical Implications. *Earth and Planetary Science Letters*, 165(2): 187–196. [https://doi.org/10.1016/s0012-821x\(98\)00266-0](https://doi.org/10.1016/s0012-821x(98)00266-0)
- Burnard, P.G., Poly, D.A., 2004. Importance of Mantle Derived Fluids during Granite Associated Hydrothermal Circulation: He and Ar Isotopes of Ore Minerals from Panasqueira. *Geochimica et Cosmochimica Acta*, 68(7): 1607–1615. <https://doi.org/10.1016/j.gca.2003.10.008>
- Cao, S.Y., Liu, J.L., Leiss, B., et al., 2011. Oligo-Miocene Shearing along the Ailao Shan-Red River Shear Zone: Constraints from Structural Analysis and Zircon U/Pb Geochronology of Magmatic Rocks in the Diancang Shan Massif, SE Tibet, China. *Gondwana Research*, 19(4):975–993. <https://doi.org/10.1016/j.gr.2010.10.006>
- Carrier, A., Jebrak, M., Angelier, J., et al., 2000. The Silidor Deposit, Rouyn-Noranda District, Abitibi Belt: Geology, Structural Evolution, and Paleostress Modeling of an Au Quartz Vein-Type Deposit in an Archean Trondhjemite. *Economic Geology*, 95(5):1049–1065.
- Chen, M.H., Mao, J.W., Bierlein, F.P., et al., 2011. Structural Features and Metallogenesis of the Carlin-Type Jinfeng (Lannigou) Gold Deposit, Guizhou Province, China. *Ore Geology Reviews*, 43(1): 217–234. <https://doi.org/10.1016/j.oregeorev.2011.06.009>
- Chen, Y.J., Pirajno, F., Lai, Y., et al., 2004. Metallogenic Time and Tectonic Setting of the Jiaodong Gold Province, Eastern China. *Acta Petrologica Sinica*, 20(4):907–922 (in Chinese with English abstract).
- Chen, Y.J., Pirajno, F., Qi, J.P., 2008. The Shangong Gold Deposit, Eastern Qinling Orogen, China: Isotope Geochemistry and Implications for Ore Genesis. *Journal of Asian Earth Sciences*, 33(3–4): 252–266. <https://doi.org/10.1016/j.jseaes.2007.12.002>
- Chen, Y.J., Zhai, M.G., Jiang, S.Y., 2009. Significant Achievements and Open Issues in Study of Orogenesis and Metallogenesis Surrounding the North China Continent. *Acta Petrologica Sinica*, 25(11):2695–2726 (in Chinese with English abstract).
- Christie, A.B., Brathwaite, R.L., 2003. Hydrothermal Alteration in Metasedimentary Rock-Hosted Orogenic Gold Deposits, Reefton Goldfield, South Island, New Zealand. *Mineralium Deposita*, 38(1): 87–107. <https://doi.org/10.1007/s00126-002-0280-9>
- Connolly, J.A.D., Cesare, B., 1993. C-O-H-S Fluid Composition and Oxygen Fugacity in Graphitic Metapelites. *Journal of Metamorphic Geology*, 11(3): 379–388. <https://doi.org/10.1111/j.1525-1314.1993.tb00155.x>
- Cox, S.F., 2010. The Application of Failure Mode Diagrams for Exploring the Roles of Fluid Pressure and Stress States in Controlling Styles of Fracture-Controlled Permeability Enhancement in Faults and Shear Zones. *Geofluids*, 10: 217–233. <https://doi.org/10.1111/j.1468-8123.2010.00281.x>
- Cox, S.F., 2016. Injection-Driven Swarm Seismicity and Permeability Enhancement: Implications for the Dynamics of Hydrothermal Ore Systems in High Fluid-Flux, Overpressured Faulting Regimes: An Invited Paper. *Economic Geology*, 111(3): 559–587. <https://doi.org/10.2113/econgeo.111.3.559>
- Cox, S.F., 2019. The Dynamics of Permeability Enhancement and Fluid Flow in Overpressured, Fracture Controlled Hydrothermal Systems. *Economic Geology* (in press).
- Cox, S.F., Etheridge, M.A., Cas, R.A.F., et al., 1991. Deformational Style of the Castlemaine Area, Bendigo-Ballarat Zone: Implications for Evolution of Crustal Structure in Central Victoria. *Australian Journal of Earth Sciences*, 38(2):151–170.
- Dai, J.G., Wang, C.S., Li, Y.L., 2012. Relicts of the Early Cretaceous Seamounts in the Central-Western Yalung Zangbo Suture Zone, Southern Tibet. *Journal of Asian Earth Sciences*, 53: 25–37. <https://doi.org/10.1016/j.jseaes.2011.12.024>
- Davis, G.A., Darby, B.J., Zheng, Y.D., et al., 2002. Geometric and Temporal Evolution of an Extensional Detachment Fault, Hohhot Metamorphic Core Complex, Inner Mongolia, China. *Geology*, 30(11):1003–1006.
- De Boorder, H., 2012. Spatial and Temporal Distribution of the Orogenic Gold Deposits in the Late Palaeozoic Variscides and Southern Tianshan: How Orogenic are They? *Ore Geology Reviews*, 46: 1–31. <https://doi.org/10.1016/j.oregeorev.2012.01.002>
- Deng, J., Liu, X.F., Wang, Q.F., et al., 2015a. Origin of the Jiaodong-Type Xinli Gold Deposit, Jiaodong Peninsula, China: Constraints from Fluid Inclusion and C-D-O-S-Sr Isotope Compositions. *Ore Geology Reviews*, 65: 674–

686. <https://doi.org/10.1016/j.oregeorev.2014.04.018>
- Deng, J., Wang, Q.F., Li, G.J., et al., 2015b. Structural Control and Genesis of the Oligocene Zhenyuan Orogenic Gold Deposit, SW China. *Ore Geology Reviews*, 65:42—54. <https://doi.org/10.1016/j.oregeorev.2014.08.002>
- Deng, J., Wang, C.M., Bagas, L., et al., 2015c. Cretaceous-Cenozoic Tectonic History of the Jiaojia Fault and Gold Mineralization in the Jiaodong Peninsula, China: Constraints from Zircon U-Pb, Illite K-Ar, and Apatite Fission Track Thermochronometry. *Mineralium Deposita*, 50(8): 987—1006. <https://doi.org/10.1007/s00126-015-0584-1>
- Deng, J., Wang, Q.F., 2016. Gold Mineralization in China: Metallogenic Provinces, Deposit Types and Tectonic Framework. *Gondwana Research*, 36:219—274. <https://doi.org/10.1016/j.gr.2015.10.003>
- Deng, J., Wang, Q.F., Li, G.J., et al., 2014a. Tethys Tectonic Evolution and Its Bearing on the Distribution of Important Mineral Deposits in the Sanjiang Region, SW China. *Gondwana Research*, 26(2): 419—437. <https://doi.org/10.1016/j.gr.2013.08.002>
- Deng, J., Wang, Q.F., Li, G.J., et al., 2014b. Cenozoic Tectono-Magmatic and Metallogenic Processes in the Sanjiang Region, Southwestern China. *Earth - Science Reviews*, 138: 268—299. <https://doi.org/10.1016/j.earsci-rev.2014.05.015>
- Deng, J., Yuan, W.M., Carranza, E.J.M., et al., 2014c. Geochronology and Thermochronometry of the Jiapigou Gold Belt, Northeastern China: New Evidence for Multiple Episodes of Mineralization. *Journal of Asian Earth Sciences*, 89:10—27.
- Deng, J., Wang, Q.F., Wan, L., et al., 2009a. Self-Similar Fractal Analysis of Gold Mineralization of Dayingezhuang Disseminated-Veinlet Deposit in Jiaodong Gold Province, China. *Journal of Geochemical Exploration*, 102(2):95—102.
- Deng, J., Yang, L.Q., Gao, B.F., et al., 2009b. Fluid Evolution and Metallogenic Dynamics during Tectonic Regime Transition: Example from the Jiapigou Gold Belt in Northeast China. *Resource Geology*, 59(2): 140—152. <https://doi.org/10.1111/j.1751-3928.2009.00086.x>
- Deng, J., Wang, Q.F., Wan, L., et al., 2011. A Multifractal Analysis of Mineralization Characteristics of the Dayingezhuang Disseminated-Veinlet Gold Deposit in the Jiaodong Gold Province of China. *Ore Geology Reviews*, 40(1):54—64.
- Deng, J., Wang, Q.F., Yang, L.Q., et al., 2010a. Delineation and Explanation of Geochemical Anomalies Using Fractal Models in the Heqing Area, Yunnan Province, China. *Journal of Geochemical Exploration*, 105(3): 95—105. <https://doi.org/10.1016/j.gexplo.2010.04.005>
- Deng, J., Yang, L.Q., Sun, Z.S., et al., 2010b. A Metallogenic Model of Gold Deposits of the Jiaodong Granite-Greenstone Belt. *Acta Geologica Sinica (English Edition)*, 77(4):537—546.
- Deng, J., Yang, L.Q., Wang, C.M., 2011. Research Advances of Superimposed Orogenesis and Metallogenesis in the Sanjiang Tethys. *Acta Petrologica Sinica*, 27(9):2501—2509(in Chinese with English abstract).
- Ding, Q.F., Jiang, S.Y., Sun, F.Y., 2014. Zircon U-Pb Geochronology, Geochemical and Sr-Nd-Hf Isotopic Compositions of the Triassic Granite and Diorite Dikes from the Wulonggou Mining Area in the Eastern Kunlun Orogen, NW China: Petrogenesis and Tectonic Implications. *Lithos*, 205: 266—283. <https://doi.org/10.1016/j.lithos.2014.07.015>
- Drummond, B.J., Goleby, B.R., Swager, C.P., et al., 1993. Constraints on Archean Crustal Composition and Structure Provided by Deep Seismic Sounding in the Yilgarn Block. *Ore Geology Reviews*, 8(1—2):117—124.
- Du, J.X., Zhang, L.F., Bader, T., et al., 2014. Metamorphic Evolution of Ultrahigh-Pressure Rocks from Chinese Southwestern Tianshan and a Possible Indicator of UHP-Metamorphism Using Garnet Composition in Low-*T* Eclogites. *Journal of Asian Earth Sciences*, 91: 69—88. <https://doi.org/10.1016/j.jseaes.2014.04.010>
- Dziggel, A., Poujol, M., Otto, A., et al., 2010. New U-Pb and ⁴⁰Ar/³⁹Ar Ages from the Northern Margin of the Barberton Greenstone Belt, South Africa: Implications for the Formation of Mesoarchean Gold Deposits. *Precambrian Research*, 179(1—4):206—220. <https://doi.org/10.1016/j.precamres.2010.03.006>
- Eisenlohr, B.N., Groves, D.I., Partington, G.A., 1989. Crustal-Scale Shear Zones and Their Significance to Archean Gold Mineralization in Western Australia. *Mineralium Deposita*, 24(1):1—8.
- Elmer, F.L., White, R.W., Powell, R., 2006. Devolatilization of Metabasic Rocks during Greenschist-Amphibolite Facies Metamorphism. *Journal of Metamorphic Geology*, 24(6): 497—513. <https://doi.org/10.1111/j.1525-1314.2006.00650.x>
- Evans, K.A., 2010. A Test of the Viability of Fluid-Wall Rock Interaction Mechanisms for Changes in Opaque Phase Assemblage in Metasedimentary Rocks in the Kambalda-St. Ives Goldfield, Western Australia. *Mineralium Deposita*, 45(2):207—213.

- Evans, K.A., Phillips, G.N., Powell, R., 2006. Rock-Buffering of Auriferous Fluids in Altered Rocks Associated with the Golden Mile-Style Mineralization, Kalgoorlie Gold Field, Western Australia. *Economic Geology*, 101(4): 805–817. <https://doi.org/10.2113/gsecongeo.101.4.805>
- Fan, H.R., Zhai, M.G., Xie, Y.H., et al., 2003. Ore-Forming Fluids Associated with Granite-Hosted Gold Mineralization at the Sanshandao Deposit, Jiaodong Gold Province, China. *Mineralium Deposita*, 38(6):739–750. <https://doi.org/10.1007/s00126-003-0368-x>
- Finch, E.G., Tomkins, A.G., 2017. Pyrite-Pyrrhotite Stability in a Metamorphic Aureole: Implications for Orogenic Gold Genesis. *Economic Geology*, 112(3): 661–674. <https://doi.org/10.2113/econgeo.112.3.661>
- Finlay, A. J., Selby, D., Osborne, M. J., et al., 2010. Fault-Charged Mantle-Fluid Contamination of United Kingdom North Sea Oils: Insights from Re-Os Isotopes. *Geology*, 38(11): 979–982. <https://doi.org/10.1130/g31201.1>
- Fridovsky, V. Y., 2017. Structural Control of Orogenic Gold Deposits of the Verkhoyansk-Kolyma Folded Region, Northeast Russia. *Ore Geology Reviews*, 103: 38–55. <https://doi.org/10.1016/j.oregeorev.2017.01.006>
- Fu, B., Touret, J.L.R., 2014. From Granulite Fluids to Quartz-Carbonate Megashar Zones: The Gold Rush. *Geoscience Frontiers*, 5(5): 747–758. <https://doi.org/10.1016/j.gsf.2014.03.013>
- Gao, L., Wang, Q.F., Deng, J., et al., 2018. Relationship between Orogenic Gold Mineralization and Crustal Shearing along Ailaoshan-Red River Belt, Southeastern Tibetan Plateau: New Constraint from Paleomagnetism. *Geochemistry, Geophysics, Geosystems*, 19(7): 2225–2242. <https://doi.org/10.1029/2018gc007493>
- Gebre-Mariam, M., Hagemann, S.G., Groves, D.I., 1995. A Classification Scheme for Epigenetic Archaean Lode-Gold Deposits. *Mineralium Deposita*, 30(5):408–410.
- Goldfarb, R.J., Baker, T., Dube, B., et al., 2005. Distribution, Character, and Genesis of Gold Deposits in Metamorphic Belts. In: Hedenquist, J.W., Thompson, J.F.H., Goldfarb, J., eds., *Economic Geology 100th Anniversary Volume*. Society of Economic Geologists, Littleton, Colorado, USA, 407–450.
- Goldfarb, R.J., Groves, D.I., 2015. Orogenic Gold: Common or Evolving Fluid and Metal Sources through Time. *Lithos*, 233:2–26. <https://doi.org/10.1016/j.lithos.2015.07.011>
- Goldfarb, R.J., Groves, D.I., Gardoll, S., 2001. Orogenic Gold and Geologic Time: A Global Synthesis. *Ore Geology Reviews*, 18(1–2):1–75. [https://doi.org/10.1016/s0169-1368\(01\)00016-6](https://doi.org/10.1016/s0169-1368(01)00016-6)
- Goldfarb, R. J., Hart, C., Davis, G., et al., 2007. East Asian Gold: Deciphering the Anomaly of Phanerozoic Gold in Precambrian Cratons. *Economic Geology*, 102(3): 341–345. <https://doi.org/10.2113/gsecongeo.102.3.341>
- Goldfarb, R. J., Santosh, M., 2014. The Dilemma of the Jiaodong Gold Deposits: Are They Unique? *Geoscience Frontiers*, 5(2): 139–153. <https://doi.org/10.1016/j.gsf.2013.11.001>
- Griffin, W.L., Begg, G.C., O'Reilly, S.Y., 2013. Continental-Root Control on the Genesis of Magmatic Ore Deposits. *Nature Geoscience*, 6(11): 905–910. <https://doi.org/10.1038/ngeo1954>
- Groves, D., Barnicoat, A. C., Barley, M., et al., 1992. Sub-Greenschist to Granulite-Hosted Archaean Lode-Gold Deposits of the Yilgarn Craton: A Depositional Continuum from Deep-Sourced Hydrothermal Fluids in Crustal-scale Plumbing Systems. Geology Department (Key Centre) and University Extension. The University of Western Australia Publication, Perth, Australia, 325–338.
- Groves, D.I., 1993. The Crustal Continuum Model for Late-Archaean Lode-Gold Deposits of the Yilgarn Block, Western Australia. *Mineralium Deposita*, 28(6): 366–374.
- Groves, D.I., Condie, K.C., Goldfarb, R.J., et al., 2005. 100th Anniversary Special Paper: Secular Changes in Global Tectonic Processes and Their Influence on the Temporal Distribution of Gold-Bearing Mineral Deposits. *Economic Geology*, 100(2):203–224. <https://doi.org/10.2113/gsecongeo.100.2.203>
- Groves, D.I., Goldfarb, R.J., Gebre-Mariam, M., et al., 1998. Orogenic Gold Deposits: A Proposed Classification in the Context of Their Crustal Distribution and Relationship to Other Gold Deposit Types. *Ore Geology Reviews*, 13(1–5): 7–27. [https://doi.org/10.1016/s0169-1368\(97\)00012-7](https://doi.org/10.1016/s0169-1368(97)00012-7)
- Groves, D.I., Goldfarb, R.J., Robert, F., et al., 2003. Gold Deposits in Metamorphic Belts: Overview of Current Understanding, Outstanding Problems, Future Research, and Exploration Significance. *Economic Geology*, 98(1): 1–29. <https://doi.org/10.2113/gsecongeo.98.1.1>
- Groves, D.I., Santosh, M., 2015. Province-Scale Commonalities of Some World-Class Gold Deposits: Implications for Mineral Exploration. *Geoscience Frontiers*, 6(3):389–399. <https://doi.org/10.1016/j.gsf.2014.12.007>
- Groves, D. I., Santosh, M., 2016. The Giant Jiaodong Gold Province: The Key to a Unified Model for Orogenic Gold Deposits? *Geoscience Frontiers*, 7(3):409–417.

- Groves, D. I., Santosh, M., Deng, J., et al., 2019. A Holistic Model for the Origin of Orogenic Gold Deposits and Its Implications for Exploration. *Mineralium Deposita*. <https://doi.org/10.1007/s00126-019-0087-5>.
- Groves, D. I., Santosh, M., Goldfarb, R. J., et al., 2018. Structural Geometry of Orogenic Gold Deposits: Implications for Exploration of World-Class and Giant Deposits. *Geoscience Frontiers*, 9(4):1163–1177.
- Gumiel, P., Sanderson, D. J., Arias, M., et al., 2010. Analysis of the Fractal Clustering of Ore Deposits in the Spanish Iberian Pyrite Belt. *Ore Geology Reviews*, 38(4): 307–318. <https://doi.org/10.1016/j.oregeorev.2010.08.001>
- Guo, Z. F., Wilson, M., Zhang, M. L., et al., 2013. Post-Collisional, K-Rich Mafic Magmatism in South Tibet: Constraints on Indian Slab-to-Wedge Transport Processes and Plateau Uplift. *Contributions to Mineralogy and Petrology*, 165(6): 1311–1340. <https://doi.org/10.1007/s00410-013-0860-y>
- Haddad-Martim, P. M., Carranza, E. J. M., de Souza Filho, C. R., 2018. The Fractal Nature of Structural Controls on Ore Formation: The Case of the Iron Oxide Copper-Gold Deposits in the Carajás Mineral Province, Brazilian Amazon. *Economic Geology*, 113(7): 1499–1524. <https://doi.org/10.5382/econgeo.2018.4600>
- Harrison, T. M., Yin, A., Grove, M., et al., 2000. The Zedong Window: A Record of Superposed Tertiary Convergence in Southeastern Tibet. *Journal of Geophysical Research: Solid Earth*, 105(B8): 19211–19230. <https://doi.org/10.1029/2000jb900078>
- Hart, C., 2005. Classifying, Distinguishing and Exploring for Intrusion-Related Gold Systems. *The Gangue*, 87(1):9.
- Helt, K. M., Williams-Jones, A. E., Clark, J. R., et al., 2014. Constraints on the Genesis of the Archean Oxidized, Intrusion-Related Canadian Malartic Gold Deposit, Quebec, Canada. *Economic Geology*, 109(3): 713–735. <https://doi.org/10.2113/econgeo.109.3.713>
- Hodkiewicz, P. F., Groves, D. I., Davidson, G. J., et al., 2009. Influence of Structural Setting on Sulphur Isotopes in Archean Orogenic Gold Deposits, Eastern Goldfields Province, Yilgarn, Western Australia. *Mineralium Deposita*, 44(2): 129–150. <https://doi.org/10.1007/s00126-008-0211-5>
- Hou, Z. Q., Cook, N. J., 2009. Metallogeneses of the Tibetan Collisional Orogen: A Review and Introduction to the Special Issue. *Ore Geology Reviews*, 36(1–3): 2–24. <https://doi.org/10.1016/j.oregeorev.2009.05.001>
- Hou, Z. Q., Duan, L. F., Lu, Y. J., et al., 2015. Lithospheric Architecture of the Lhasa Terrane and Its Control on Ore Deposits in the Himalayan-Tibetan Orogen. *Economic Geology*, 110(6): 1541–1575. <https://doi.org/10.2113/econgeo.110.6.1541>
- Hou, Z. Q., Zaw, K., Pan, G. T., et al., 2007. Sanjiang Tethyan Metallogenesis in S. W. China: Tectonic Setting, Metallogenic Epochs and Deposit Types. *Ore Geology Reviews*, 31(1–4): 48–87. <https://doi.org/10.1016/j.oregeorev.2004.12.007>
- Hronsky, J. M. A., Groves, D. I., Loucks, R. R., et al., 2012. A Unified Model for Gold Mineralisation in Accretionary Orogens and Implications for Regional-Scale Exploration Targeting Methods. *Mineralium Deposita*, 47(4): 339–358. <https://doi.org/10.1007/s00126-012-0402-y>
- Hyndman, R. D., McCrory, P. A., Wech, A., et al., 2015. Cascadia Subducting Plate Fluids Channelled to Fore-Arc Mantle Corner: ETS and Silica Deposition. *Journal of Geophysical Research: Solid Earth*, 120(6): 4344–4358. <https://doi.org/10.1002/2015jb011920>
- Jia, S. S., Wang, E. D., Fu, J. F., et al., 2018. Indosinian Gold Mineralization and Magmatic-Hydrothermal Evolution of the Hadamengou Gold Deposit at the Northern Margin of the North China Craton: Constraints from K-Feldspar Laser $^{40}\text{Ar}/^{39}\text{Ar}$ Dating. *Journal of Geochemical Exploration*, 190: 314–324. <https://doi.org/10.1016/j.gexplo.2018.04.002>
- Jiang, S. H., Nie, F. J., Hu, P., et al., 2009. Mayum: An Orogenic Gold Deposit in Tibet, China. *Ore Geology Reviews*, 36(1–3): 160–173. <https://doi.org/10.1016/j.oregeorev.2009.03.006>
- Katayama, I., Terada, T., Okazaki, K., et al., 2012. Episodic Tremor and Slow Slip Potentially Linked to Permeability Contrasts at the Moho. *Nature Geoscience*, 5(10): 731–734. <https://doi.org/10.1038/ngeo1559>
- Kawano, S., Katayama, I., Okazaki, K., 2011. Permeability Anisotropy of Serpentine and Fluid Pathways in a Subduction Zone. *Geology*, 39(10): 939–942. <https://doi.org/10.1130/g32173.1>
- Kennedy, B. M., 1997. Mantle Fluids in the San Andreas Fault System, California. *Science*, 278(5341): 1278–1281.
- Kennedy, B. M., van Soest, M. C., 2007. Flow of Mantle Fluids through the Ductile Lower Crust: Helium Isotope Trends. *Science*, 318(5855): 1433–1436.
- Kerrick, R., Fyfe, W. S., 1981. The Gold: Carbonate Association, Source of CO_2 , and CO_2 Fixation Reactions in Archean Lode Deposits. *Chemical Geology*, 33(1–4): 265–294.
- Kerrick, R., Goldfarb, R., Groves, D., et al., 2000. The Charac-

- teristics, Origins, and Geodynamic Settings of Supergiant Gold Metallogenic Provinces. *Science in China (Series D)*, 43(Suppl.1):1–68.
- Kerrich, R., Wyman, D., 1990. Geodynamic Setting of Mesothermal Gold Deposits: An Association with Accretionary Tectonic Regimes. *Geology*, 18(9):882–825.
- Klein-Ben David, O., Pettko, T., Kessel, R., 2011. Chromium Mobility in Hydrous Fluids at Upper Mantle Conditions. *Lithos*, 125(1–2):122–130.
- Klemperer, S. L., Kennedy, B. M., Sastry, S. R., et al., 2013. Mantle Fluids in the Karakoram Fault: Helium Isotope Evidence. *Earth and Planetary Science Letters*, 366:59–70. <https://doi.org/10.1016/j.epsl.2013.01.013>
- Knight, J. T., Groves, D. I., Ridley, J. R., 1993. The Coolgardie Goldfield, Western Australia: District-Scale Controls on an Archaean Gold Camp in an Amphibolite Facies Terrane. *Mineralium Deposita*, 28(6):436–456.
- Knight, J. T., Ridley, J. R., Groves, D. I., 2000. The Archaean Amphibolite Facies Coolgardie Goldfield, Yilgarn Craton, Western Australia: Nature, Controls, and Gold Field-Scale Patterns of Hydrothermal Wall-Rock Alteration. *Economic Geology*, 95(1): 49–84. <https://doi.org/10.2113/gsecongeo.95.1.49>
- Kolb, J., Dziggel, A., Bagas, L., 2015. Hypozonal Lode Gold Deposits: A Genetic Concept Based on a Review of the New Consort, Renco, Hutti, Hira Buddini, Navachab, Nevoria and the Granites Deposits. *Precambrian Research*, 262: 20–44. <https://doi.org/10.1016/j.precamres.2015.02.022>
- Kolb, J., Kisters, A. F. M., Hoernes, S., et al., 2000. The Origin of Fluids and Nature of Fluid-Rock Interaction in Mid-Crustal Auriferous Mylonites of the Renco Mine, Southern Zimbabwe. *Mineralium Deposita*, 35(2–3): 109–125. <https://doi.org/10.1007/s001260050010>
- Kolb, J., Meyer, M. F., 2002. Fluid Inclusion Record of the Hypozonal Orogenic Renco Gold Deposit (Zimbabwe) during the Retrograde *P-T* Evolution. *Contributions to Mineralogy and Petrology*, 143(4): 495–509. <https://doi.org/10.1007/s00410-002-0360-y>
- Kolb, J., Rogers, A., Meyer, F. M., 2005. Relative Timing of Deformation and Two-Stage Gold Mineralization at the Hutti Mine, Dharwar Craton, India. *Mineralium Deposita*, 40(2):156–174.
- Kontak, D. J., Smith, P. K., Kerrich, R., et al., 1990. Integrated Model for Meguma Group Lode Gold Deposits, Nova Scotia, Canada. *Geology*, 18(3):238–242.
- LaFlamme, C., Jamieson, J. W., Fiorentini, M. L., et al., 2018. Investigating Sulfur Pathways through the Lithosphere by Tracing Mass Independent Fractionation of Sulfur to the Lady Bountiful Orogenic Gold Deposit, Yilgarn Craton. *Gondwana Research*, 58: 27–38. <https://doi.org/10.1016/j.gr.2018.02.005>
- Large, R. R., Bull, S. W., Maslennikov, V. V., 2011. A Carbonaceous Sedimentary Source-Rock Model for Carlin-Type and Orogenic Gold Deposits. *Economic Geology*, 106(3): 331–358. <https://doi.org/10.2113/econgeo.106.3.331>
- Large, R. R., Danyushevsky, L., Hollit, C., et al., 2009. Gold and Trace Element Zonation in Pyrite Using a Laser Imaging Technique: Implications for the Timing of Gold in Orogenic and Carlin-Style Sediment-Hosted Deposits. *Economic Geology*, 104(5): 635–668. <https://doi.org/10.2113/gsecongeo.104.5.635>
- Large, R. R., Maslennikov, V. V., Robert, F., et al., 2007. Multistage Sedimentary and Metamorphic Origin of Pyrite and Gold in the Giant Sukhoi Log Deposit, Lena Gold Province, Russia. *Economic Geology*, 102(7): 1233–1267. <https://doi.org/10.2113/gsecongeo.102.7.1233>
- Lawrence, D. M., Treloar, P. J., Rankin, A. H., et al., 2013. The Geology and Mineralogy of the Loulo Mining District, Mali, West Africa: Evidence for Two Distinct Styles of Orogenic Gold Mineralization. *Economic Geology*, 108(2): 199–227. <https://doi.org/10.2113/econgeo.108.2.199>
- Lebrun, E., Miller, J., Thébaud, N., et al., 2017. Structural Controls on an Orogenic Gold System: The World-Class Siguiri Gold District, Siguiri Basin, Guinea, West Africa. *Economic Geology*, 112(1): 73–98. <https://doi.org/10.2113/econgeo.112.1.73>
- Li, H. J., Wang, Q. F., Deng, J., et al., 2019a. Alteration and Mineralization Styles of the Orogenic Disseminated Zhenyuan Gold Deposit, Southeastern Tibet: Contrast with Carlin Gold Deposit. *Geoscience Frontiers*. <https://doi.org/10.1016/j.gsf.2019.01.008>
- Li, H. J., Wang, Q. F., Groves, D. I., et al., 2019b. Alteration of Eocene Lamprophyres in the Zhenyuan Orogenic Gold Deposit, Yunnan Province, China: Composition and Evolution of Ore Fluids. *Ore Geology Reviews*, 107:1068–1083. <https://doi.org/10.1016/j.oregeorev.2019.03.032>
- Li, H. J., Wang, Q. F., Yang, L., et al., 2017. Orogenic Gold Deposits Formed in Tibetan Collisional Orogen Setting: Geotectonic Setting, Geological and Geochemical Features. *Acta Petrologica Sinica*, 33(7):2189–2201 (in Chinese with English abstract).
- Li, J. F., Xia, B., Liu, L. W., et al., 2009. SHRIMP U-Pb Dating for the Gabbro in Qunrang Ophiolite, Tibet: The Geo-

- chronology Constraint for the Development of Eastern Tethys Basin. *Geotectonica et Metallogenia*, 33(2): 294—298.
- Li, J. W., Bi, S. J., Selby, D., et al., 2012a. Giant Mesozoic Gold Provinces Related to the Destruction of the North China Craton. *Earth and Planetary Science Letters*, 349—350: 26—37. <https://doi.org/10.1016/j.epsl.2012.06.058>
- Li, J. W., Li, Z. K., Zhou, M. F., et al., 2012b. The Early Cretaceous Yangzhaiyu Lode Gold Deposit, North China Craton: A Link between Craton Reactivation and Gold Veining. *Economic Geology*, 107(1): 43—79.
- Li, J. W., Vasconcelos, P. M., Zhou, M. F., et al., 2006. Geochronology of the Pengjiakuang and Rushan Gold Deposits, Eastern Jiaodong Gold Province, Northeastern China: Implications for Regional Mineralization and Geodynamic Setting. *Economic Geology*, 101(5): 1023—1038. <https://doi.org/10.2113/gsecongeo.101.5.1023>
- Li, L., Santosh, M., Li, S. R., 2015. The ‘Jiaodong Type’ Gold Deposits: Characteristics, Origin and Prospecting. *Ore Geology Reviews*, 65: 589—611. <https://doi.org/10.1016/j.oregeorev.2014.06.021>
- Li, Q. L., Chen, F. K., Yang, J. H., et al., 2008. Single Grain Pyrite Rb-Sr Dating of the Linglong Gold Deposit, Eastern China. *Ore Geology Reviews*, 34(3): 263—270. <https://doi.org/10.1016/j.oregeorev.2007.10.003>
- Li, S. H., Zhang, J., Deng, J., et al., 2011. The Characteristics of Ore-Forming Fluid and Genetic Type of the Chang’an Gold Deposit in Southern Ailaoshan Metallogenic Belt. *Acta Petrologica Sinica*, 27(12): 3777—3786 (in Chinese with English abstract).
- Li, X. F., Mao, J. W., Wang, C. Z., et al., 2007. The Daduhe Gold Field at the Eastern Margin of the Tibetan Plateau: He, Ar, S, O, and H Isotopic Data and Their Metallogenic Implications. *Ore Geology Reviews*, 30(3—4): 244—256. <https://doi.org/10.1016/j.oregeorev.2005.10.005>
- Liang, Y. H., Sun, X. M., Shi, G. Y., et al., 2011. Ore-Forming Fluid Geochemistry and Genesis of Laowangzhai Large Scale Orogenic Gold Deposit in Ailaoshan Gold Belt, Yunnan Province, China. *Acta Petrologica Sinica*, 27(9): 2533—2540 (in Chinese with English abstract).
- Lin, T. H., Chung, S. L., Chiu, H. Y., et al., 2012. Zircon U-Pb and Hf Isotope Constraints from the Ailao Shan - Red River Shear Zone on the Tectonic and Crustal Evolution of Southwestern China. *Chemical Geology*, 291(1): 23—37. <https://doi.org/10.1016/j.chemgeo.2011.11.011>
- Liu, J. J., Liu, C. H., Carranza, E. J. M., et al., 2015a. Geological Characteristics and Ore-Forming Process of the Gold Deposits in the Western Qinling Region, China. *Journal of Asian Earth Sciences*, 103: 40—69. <https://doi.org/10.1016/j.jseaes.2014.11.012>
- Liu, H. C., Wang, Y. J., Cawood, P. A., et al., 2015b. Record of Tethyan Ocean Closure and Indosinian Collision along the Ailaoshan Suture Zone (SW China). *Gondwana Research*, 27(3): 1292—1306. <https://doi.org/10.1016/j.gr.2013.12.013>
- Liu, W., Fei, P. X., 2006. Methane-Rich Fluid Inclusions from Ophiolitic Dunite and Post-Collisional Mafic-Ultramafic Intrusion: The Mantle Dynamics underneath the Palaeo-Asian Ocean through to the Post-Collisional Period. *Earth and Planetary Science Letters*, 242(3—4): 286—301. <https://doi.org/10.1016/j.epsl.2005.11.059>
- MacKenzie, D. J., Craw, D., Begbie, M., 2007. Mineralogy, Geochemistry, and Structural Controls of a Disseminated Gold-Bearing Alteration Halo around the Schist-Hosted Bullendale Orogenic Gold Deposit, New Zealand. *Journal of Geochemical Exploration*, 93(3): 160—176.
- Malpas, J., Zhou, M. F., Robinson, P. T., et al., 2003. Geochemical and Geochronological Constraints on the Origin and Emplacement of the Yarlung Zangbo Ophiolites, Southern Tibet. *Geological Society, London, Special Publications*, 218(1): 191—206. <https://doi.org/10.1144/gsl.sp.2003.218.01.11>
- Mao, J. W., Pirajno, F., Xiang, J. F., et al., 2011. Mesozoic Molybdenum Deposits in the East Qinling-Dabie Orogenic Belt: Characteristics and Tectonic Settings. *Ore Geology Reviews*, 43(1): 264—293. <https://doi.org/10.1016/j.oregeorev.2011.07.009>
- Mao, J. W., Qiu, Y. M., Goldfarb, R. J., et al., 2002. Geology, Distribution, and Classification of Gold Deposits in the Western Qinling Belt, Central China. *Mineralium Deposita*, 37(3—4): 352—377.
- Mao, J. W., Wang, Y. T., Li, H. M., et al., 2008. The Relationship of Mantle-Derived Fluids to Gold Metallogenesis in the Jiaodong Peninsula: Evidence from D-O-C-S Isotope Systematics. *Ore Geology Reviews*, 33(3—4): 361—381. <https://doi.org/10.1016/j.oregeorev.2007.01.003>
- Mao, J. W., Xie, G. Q., Li, X. F., et al., 2004. Mesozoic Large Scale Mineralization and Multiple Lithospheric Extension in South China. *Earth Science Frontiers*, 11(1): 45—55 (in Chinese with English abstract).
- Mao, J. W., Xie, G. Q., Zhang, Z. H., et al., 2005. Mesozoic Large-Scale Metallogenic Pulses in North China and Corresponding Geodynamic Settings. *Acta Petrologica Sinica*, 21(1): 169—188 (in Chinese with English abstract).

- McNaughton, N. J., Groves, D. I., Witt, W. K., 1993. The Source of Lead in Archaean Lode Gold Deposits of the Menzies-Kalgoorlie-Kambalda Region, Yilgarn Block, Western Australia. *Mineralium Deposita*, 28(6): 495–502.
- Mernagh, T. P., Bierlein, F. P., 2008. Transport and Precipitation of Gold in Phanerozoic Metamorphic Terranes from Chemical Modeling of Fluid-Rock Interaction. *Economic Geology*, 103(8): 1613–1640. <https://doi.org/10.2113/gsecongeo.103.8.1613>
- Morelli, R., Creaser, R. A., Seltmann, R., et al., 2007. Age and Source Constraints for the Giant Muruntau Gold Deposit, Uzbekistan, from Coupled Re-Os-He Isotopes in Arsenopyrite. *Geology*, 35(9): 795–798.
- Müller, D., Groves, D. I., 1997. Indirect Associations between Lamprophyres and Gold-Copper Deposits. In: Müller, D., Groves, D. I., eds., Potassic Igneous Rocks and Associated Gold-Copper Mineralization. Springer, Berlin, Heidelberg, 143–166.
- Munro, M. A., Ord, A., Hobbs, B. E., 2018. Spatial Organization of Gold and Alteration Mineralogy in Hydrothermal Systems: Wavelet Analysis of Drillcore from Sunrise Dam Gold Mine, Western Australia. *Geological Society, London, Special Publications*, 453(1): 165–204. <https://doi.org/10.1144/sp453.10>
- Nesbitt, B. E., 1991. Phanerozoic Gold Deposits in Tectonically Active Continental Margins. In: Nesbitt, B. E., ed., Gold Metallogeny and Exploration. Springer, Boston, MA, 104–132.
- Peacock, S. A., 1990. Fluid Processes in Subduction Zones. *Science*, 248(4953): 329–337. <https://doi.org/10.1126/science.248.4953.329>
- Peacock, S. M., Christensen, N. I., Bostock, M. G., et al., 2011. High Pore Pressures and Porosity at 35 km Depth in the Cascadia Subduction Zone. *Geology*, 39(5): 471–474. <https://doi.org/10.1130/g31649.1>
- Phillips, G. N., Powell, R., 1993. Link between Gold Provinces. *Economic Geology*, 88(5): 1084–1098. <https://doi.org/10.2113/gsecongeo.88.5.1084>
- Phillips, G. N., Powell, R., 2009. Formation of Gold Deposits: Review and Evaluation of the Continuum Model. *Earth-Science Reviews*, 94(1–4): 1–21. <https://doi.org/10.1016/j.earscirev.2009.02.002>
- Phillips, G. N., Powell, R., 2010. Formation of Gold Deposits: A Metamorphic Devolatilization Model. *Journal of Metamorphic Geology*, 28(6): 689–718.
- Phillips, G. N., Powell, R., 2015. A Practical Classification of Gold Deposits, with a Theoretical Basis. *Ore Geology Reviews*, 65: 568–573. <https://doi.org/10.1016/j.oregeorev.2014.04.006>
- Pili, É., Kennedy, B. M., Conrad, M. E., et al., 2011. Isotopic Evidence for the Infiltration of Mantle and Metamorphic CO₂-H₂O Fluids from below in Faulted Rocks from the San Andreas Fault System. *Chemical Geology*, 281(3–4): 242–252. <https://doi.org/10.1016/j.chemgeo.2010.12.011>
- Pitcairn, I. K., Craw, D., Teagle, D. A. H., 2015. Metabasalts as Sources of Metals in Orogenic Gold Deposits. *Mineralium Deposita*, 50(3): 373–390. doi: 10.1007/s00126-014-0547-y
- Pitcairn, I. K., Teagle, D. A. H., Craw, D., et al., 2006. Sources of Metals and Fluids in Orogenic Gold Deposits: Insights from the Otago and Alpine Schists, New Zealand. *Economic Geology*, 101(8): 1525–1546. <https://doi.org/10.2113/gsecongeo.101.8.1525>
- Ridley, J. R., Diamond, L. W., 2000. Fluid Chemistry of Orogenic Lode Gold Deposits and Implications for Genetic Models. *Reviews in Economic Geology*, 13: 141–162.
- Romer, R. L., Kroner, U., 2018. Paleozoic Gold in the Appalachians and Variscides. *Ore Geology Reviews*, 92: 475–505. <https://doi.org/10.1016/j.oregeorev.2017.11.021>
- Rospabé, M., Ceuleneer, G., Benoit, M., et al., 2017. Origin of the Dunitic Mantle-Crust Transition Zone in the Oman Ophiolite: The Interplay between Percolating Magmas and High-Temperature Hydrous Fluids. *Geology*, 45(5): 471–474. <https://doi.org/10.1130/g38778.1>
- Saager, R., Meyer, M., Muff, R., 1982. Gold Distribution in Supracrustal Rocks from Archean Greenstone Belts of Southern Africa and from Paleozoic Ultramafic Complexes of the European Alps; Metallogenic and Geochemical Implications. *Economic Geology*, 77(1): 1–24. <https://doi.org/10.2113/gsecongeo.77.1.1>
- Sack, P. J., Large, R. R., Gregory, D. D., 2018. Geochemistry of Shale and Sedimentary Pyrite as a Proxy for Gold Fertility in the Selwyn Basin Area, Yukon. *Mineralium Deposita*, 53(7): 997–1018. <https://doi.org/10.1007/s00126-018-0793-5>
- Safonov, Y. G., 2010. Topical Issues of the Theory of Gold Deposit Formation. *Geology of Ore Deposits*, 52(6): 438–458.
- Sarma, D. S., Fletcher, I. R., Rasmussen, B., et al., 2011. Archaean Gold Mineralization Synchronous with Late Cratonization of the Western Dharwar Craton, India: 2.52 Ga U-Pb Ages of Hydrothermal Monazite and Xenotime in Gold Deposits. *Mineralium Deposita*, 46(3): 273–288.
- Sausse, J., Jacquot, E., Fritz, B., et al., 2001. Evolution of

- Crack Permeability during Fluid-Rock Interaction. Example of the Brézouard Granite (Vosges, France). *Tectonophysics*, 336(1-4): 199-214. [https://doi.org/10.1016/s0040-1951\(01\)00102-0](https://doi.org/10.1016/s0040-1951(01)00102-0)
- Schrauder, M., Navon, O., 1994. Hydrous and Carbonatitic Mantle Fluids in Fibrous Diamonds from Jwaneng, Botswana. *Geochimica et Cosmochimica Acta*, 58(2): 761-771. [https://doi.org/10.1016/0016-7037\(94\)90504-5](https://doi.org/10.1016/0016-7037(94)90504-5)
- Selvaraja, V., Caruso, S., Fiorentini, M.L., et al., 2017. Atmospheric Sulfur in the Orogenic Gold Deposits of the Archean Yilgarn Craton, Australia. *Geology*, 45(8): 691-694.
- Seno, T., Kirby, S.H., 2014. Formation of Plate Boundaries: The Role of Mantle Volatilization. *Earth - Science Reviews*, 129: 85-99. <https://doi.org/10.1016/j.earsci-ev.2013.10.011>
- Sibson, R. H., 1996. Structural Permeability of Fluid-Driven Fault-Fracture Meshes. *Journal of Structural Geology*, 18(8): 1031-1042. [https://doi.org/10.1016/0191-8141\(96\)00032-6](https://doi.org/10.1016/0191-8141(96)00032-6)
- Sibson, R. H., 2001. Seismogenic Framework for Ore Deposition. *Reviews in Economic Geology*, 14: 25-50.
- Sibson, R. H., 2004. Controls on Maximum Fluid Overpressure Defining Conditions for Mesozonal Mineralisation. *Journal of Structural Geology*, 26(6-7): 1127-1136. <https://doi.org/10.1016/j.jsg.2003.11.003>
- Sibson, R. H., 2013. Stress Switching in Subduction Forearcs: Implications for Overpressure Containment and Strength Cycling on Megathrusts. *Tectonophysics*, 600: 142-152. <https://doi.org/10.1016/j.tecto.2013.02.035>
- Sibson, R. H., Robert, F., Poulsen, K. H., 1988. High-Angle Reverse Faults, Fluid-Pressure Cycling, and Mesothermal Gold-Quartz Deposits. *Geology*, 16(6): 551-555.
- Sibson, R. H., Scott, J., 1998. Stress / Fault Controls on the Containment and Release of Overpressured Fluids: Examples from Gold-Quartz Vein Systems in Juneau, Alaska; Victoria, Australia and Otago, New Zealand. *Ore Geology Reviews*, 13(1-5): 293-306. [https://doi.org/10.1016/s0169-1368\(97\)00023-1](https://doi.org/10.1016/s0169-1368(97)00023-1)
- Sillitoe, R.H., 1991. Intrusion-Related Gold Deposits. In: Sillitoe, R. H., ed., *Gold Metallogeny and Exploration*. Springer, Boston, MA, 165-209.
- Sillitoe, R. H., 2008. Major Gold Deposits and Belts of the North and South American Cordillera: Distribution, Tectonomagmatic Settings, and Metallogenic Considerations. *Economic Geology*, 103(4): 663-687.
- Sillitoe, R. H., Thompson, J. F. H., 1998. Intrusion-Related Vein Gold Deposits: Types, Tectono-Magmatic Settings and Difficulties of Distinction from Orogenic Gold Deposits. *Resource Geology*, 48(4): 237-250. <https://doi.org/10.1111/j.1751-3928.1998.tb00021.x>
- Song, Y., Jiang, S. H., Bagas, L., et al., 2016. The Geology and Geochemistry of Jinchangyu Gold Deposit, North China Craton: Implications for Metallogensis and Geodynamic Setting. *Ore Geology Reviews*, 73: 313-329. <https://doi.org/10.1016/j.oregeorev.2014.10.031>
- Spence-Jones, C.P., Jenkin, G.R.T., Boyce, A.J., et al., 2018. Tellurium, Magmatic Fluids and Orogenic Gold: An Early Magmatic Fluid Pulse at Cononish Gold Deposit, Scotland. *Ore Geology Reviews*, 102: 894-905. <https://doi.org/10.1016/j.oregeorev.2018.05.014>
- Standish, C.D., Dhuime, B., Chapman, R.J., et al., 2014. The Genesis of Gold Mineralisation Hosted by Orogenic Belts: A Lead Isotope Investigation of Irish Gold Deposits. *Chemical Geology*, 378-379: 40-51. <https://doi.org/10.1016/j.chemgeo.2014.04.012>
- Steadman, J.A., Large, R.R., 2016. Synsedimentary, Diagenetic, and Metamorphic Pyrite, Pyrrhotite, and Marcasite at the Homestake BIF-Hosted Gold Deposit, South Dakota, USA: Insights on Au-As Ore Genesis from Textural and LA-ICP-MS Trace Element Studies. *Economic Geology*, 111(7): 1731-1752. <https://doi.org/10.2113/econgeo.111.7.1731>
- Steadman, J.A., Large, R.R., Meffre, S., et al., 2013. Age, Origin and Significance of Nodular Sulfides in 2 680 Ma Carbonaceous Black Shale of the Eastern Goldfields Superterrane, Yilgarn Craton, Western Australia. *Precambrian Research*, 230: 227-247. <https://doi.org/10.1016/j.precamres.2013.02.013>
- Streit, J.E., Cox, S.F., 2001. Fluid Pressures at Hypocenters of Moderate to Large Earthquakes. *Journal of Geophysical Research: Solid Earth*, 106(B2): 2235-2243. <https://doi.org/10.1029/2000jb900359>
- Stüwe, K., 1998. Heat Sources of Cretaceous Metamorphism in the Eastern Alps: A Discussion. *Tectonophysics*, 287(1-4): 251-269. [https://doi.org/10.1016/s0040-1951\(98\)80072-3](https://doi.org/10.1016/s0040-1951(98)80072-3)
- Sun, X. M., Wei, H. X., Zhai, W., et al., 2014. Bangbu: The Largest Cenozoic Orogenic Gold Deposit in Southern Tibet, China. *Acta Geologica Sinica (English Edition)*, 88 (Suppl.2): 788-789.
- Sun, X. M., Wei, H. X., Zhai, W., et al., 2016. Fluid Inclusion Geochemistry and Ar-Ar Geochronology of the Cenozoic Bangbu Orogenic Gold Deposit, Southern Tibet, China. *Ore Geology Reviews*, 74: 196-210. <https://doi.org/10.1016/j.oregeorev.2015.11.021>

- Sun, X. M., Zhang, Y., Xiong, D. X., et al., 2009. Crust and Mantle Contributions to Gold-Forming Process at the Daping Deposit, Ailaoshan Gold Belt, Yunnan, China. *Ore Geology Reviews*, 36(1–3): 235–249. <https://doi.org/10.1016/j.oregeorev.2009.05.002>
- Tang, J., Zheng, Y. F., Wu, Y. B., et al., 2007. Geochronology and Geochemistry of Metamorphic Rocks in the Jiaobei Terrane: Constraints on Its Tectonic Affinity in the Sulu Orogen. *Precambrian Research*, 152(1–2): 48–82. <https://doi.org/10.1016/j.precamres.2006.09.001>
- Tang, L., Santosh, M., 2018. Neoproterozoic Granite-Greenstone Belts and Related Ore Mineralization in the North China Craton: An Overview. *Geoscience Frontiers*, 9(3): 751–768.
- Tomkins, A. G., 2010. Windows of Metamorphic Sulfur Liberation in the Crust: Implications for Gold Deposit Genesis. *Geochimica et Cosmochimica Acta*, 74(11): 3246–3259. <https://doi.org/10.1016/j.gca.2010.03.003>
- Tomkins, A. G., Grundy, C., 2009. Upper Temperature Limits of Orogenic Gold Deposit Formation: Constraints from the Granulite-Hosted Griffin's Find Deposit, Yilgarn Craton. *Economic Geology*, 104(5): 669–685. <https://doi.org/10.2113/gsecongeo.104.5.669>
- Tripp, G. I., Vearncombe, J. R., 2004. Fault / fracture Density and Mineralization: A Contouring Method for Targeting in Gold Exploration. *Journal of Structural Geology*, 26(6–7): 1087–1108. <https://doi.org/10.1016/j.jsg.2003.11.002>
- Vearncombe, J. R., 1998. Shear Zones, Fault Networks, and Archean Gold. *Geology*, 26(9): 855.
- Wall, V. J., Graupner, T., Yantsen, V., et al., 2004. Muruntau, Uzbekistan: A Giant Thermal Aureole Gold (TAG) System. In: Muhling, J., Goldfarb, R., Vielreicher, N., et al., eds., SEG 2004: Predictive Mineral Discovery Under Cover: Extended Abstracts: Centre for Global Metallogeny. University of Western Australia Publication, Perth, Australia, 199–203.
- Wang, C. S., Liu, Z. F., Hébert, R., 2000. The Yarlung-Zangbo Paleo-Ophiolite, Southern Tibet: Implications for the Dynamic Evolution of the Yarlung-Zangbo Suture Zone. *Journal of Asian Earth Sciences*, 18(6): 651–661.
- Wang, Q. F., Deng, J., Groves, D. I., Ore-controlling Structure and Genesis of Orogenic Gold Deposit with Evolving Orogenesis: Case Study from Miocene Ailaoshan Orogenic Gold Deposits, Tibet Southeastern. *Mineralium Deposita* (in review).
- Wang, Q. F., Deng, J., Liu, H., et al., 2010a. Fractal Models for Ore Reserve Estimation. *Ore Geology Reviews*, 37(1): 2–14. <https://doi.org/10.1016/j.oregeorev.2009.11.002>
- Wang, Q. F., Deng, J., Zhao, J., et al., 2010b. Tonnage-Cutoff Model and Average Grade-Cutoff Model for a Single Ore Deposit. *Ore Geology Reviews*, 38(1–2): 113–120. <https://doi.org/10.1016/j.oregeorev.2010.07.003>
- Wang, R., Richards, J. P., Zhou, L. M., et al., 2015b. The Role of Indian and Tibetan Lithosphere in Spatial Distribution of Cenozoic Magmatism and Porphyry Cu-Mo Deposits in the Gangdese Belt, Southern Tibet. *Earth-Science Reviews*, 150: 68–94.
- Wang, X. M., Shao, S. C., Wang, D. B., 2000. The Features and Geological Significance of Inclusion and Hydrogen and Oxygen Isotopes in Western Qinling Area. *Journal of Precious Metallic Geology*: 9(1): 44–48 (in Chinese with English abstract).
- Wang, Y. J., Fan, W. M., Zhang, G. W., et al., 2013. Phanerozoic Tectonics of the South China Block: Key Observations and Controversies. *Gondwana Research*, 23(4): 1273–1305. <https://doi.org/10.1016/j.gr.2012.02.019>
- Wang, Z. L., Yang, L. Q., Guo, L. N., et al., 2015a. Fluid Immiscibility and Gold Deposition in the Xincheng Deposit, Jiaodong Peninsula, China: A Fluid Inclusion Study. *Ore Geology Reviews*, 65: 701–717. <https://doi.org/10.1016/j.oregeorev.2014.06.006>
- Weatherley, D. K., Henley, R. W., 2013. Flash Vaporization during Earthquakes Evidenced by Gold Deposits. *Nature Geoscience*, 6(4): 294–298. <https://doi.org/10.1038/ngeo1759>
- Webber, A. P., Roberts, S., Taylor, R. N., et al., 2013. Golden Plumes: Substantial Gold Enrichment of Oceanic Crust during Ridge-Plume Interaction. *Geology*, 41(1): 87–90. <https://doi.org/10.1130/g33301.1>
- Weinberg, R. F., Hodkiewicz, P. F., Groves, D. I., 2004. What Controls Gold Distribution in Archean Terranes? *Geology*, 32(7): 545–548. <https://doi.org/10.1130/g20475.1>
- Weller, O. M., St-Onge, M. R., Waters, D. J., et al., 2013. Quantifying Barrovian Metamorphism in the Danba Structural Culmination of Eastern Tibet. *Journal of Metamorphic Geology*, 31(9): 909–935. <https://doi.org/10.1111/jmg.12050>
- Whitney, D. L., Teyssier, C., Fayon, A. K., 2004. Isothermal Decompression, Partial Melting and Exhumation of Deep Continental Crust. *Geological Society, London, Special Publications*, 227(1): 313–326. <https://doi.org/10.1144/gsl.sp.2004.227.01.16>
- Williams, H. M., Turner, S. P., Kelley, S., et al., 2001. Age and Composition of Dikes in Southern Tibet: New Constraints on the Timing of East-West Extension and Its

- Relationship to Postcollisional Volcanism. *Geology*, 29(4):339–342.
- Williams, H.M., Turner, S.P., Pearce, J.A., et al., 2004. Nature of the Source Regions for Post-Collisional, Potassic Magmatism in Southern and Northern Tibet from Geochemical Variations and Inverse Trace Element Modeling. *Journal of Petrology*, 45(3):555–607.
- Williams-Jones, A.E., Bowtell, R.J., Migdisov, A.A., 2009. Gold in Solution. *Elements*, 5(5):281–287.
- Wintsch, R.P., Christoffersen, R., Kronenberg, A.K., 1995. Fluid-Rock Reaction Weakening of Fault Zones. *Journal of Geophysical Research: Solid Earth*, 100(B7):13021–13032. <https://doi.org/10.1029/94jb02622>
- Wyman, D.A., 1989. Archean Shoshonitic Lamprophyres Associated with Superior Province Gold Deposits: Distribution, Tectonic Setting, Noble Metal Abundances, and Significance for Gold Mineralization. *Economic Geology Monographs*, 6:661–667.
- Wyman, D.A., Kerrich, R., 2010. Mantle Plume-Volcanic Arc Interaction: Consequences for Magmatism, Metallogeny, and Cratonization in the Abitibi and Wawa Subprovinces, Canada. *Canadian Journal of Earth Sciences*, 47(5):565–589. <https://doi.org/10.1139/e09-049>
- Wyman, D.A., O'Neill, C.O., Ayer, J.A., 2008. Evidence for Modern-Style Subduction to 3.1 Ga: A Plateau-Adakite-Gold (Diamond) Association. *The Geological Society of America*, 440:129–148.
- Yang, J.H., Wu, F.Y., Wilde, S.A., 2003. A Review of the Geodynamic Setting of Large-Scale Late Mesozoic Gold Mineralization in the North China Craton: An Association with Lithospheric Thinning. *Ore Geology Reviews*, 23(3–4):125–152. [https://doi.org/10.1016/S0169-1368\(03\)00033-7](https://doi.org/10.1016/S0169-1368(03)00033-7)
- Yang, L., Wang, Q.F., Liu, X.F., 2015. Correlation between Mineralization Intensity and Fluid-Rock Reaction in the Xinli Gold Deposit, Jiaodong Peninsula, China: Constraints from Petrographic and Statistical Approaches. *Ore Geology Reviews*, 71: 29–39. <https://doi.org/10.1016/j.oregeorev.2015.04.005>
- Yang, L., Wang, Q.F., Wang, Y.N., et al., 2018b. Proto-to Paleozoic Evolution of the Eastern Margin of Simao Block. *Gondwana Research*, 62:61–74. <https://doi.org/10.1016/j.gr.2018.02.012>
- Yang, L., Zhao, R., Wang, Q.F., et al., 2018a. Fault Geometry and Fluid-Rock Reaction: Combined Controls on Mineralization in the Xinli Gold Deposit, Jiaodong Peninsula, China. *Journal of Structural Geology*, 111:14–26. <https://doi.org/10.1016/j.jsg.2018.03.009>
- Yang, L.Q., Deng, J., Guo, C.Y., et al., 2009a. Ore-Forming Fluid Characteristics of the Dayingezhuang Gold Deposit, Jiaodong Gold Province, China. *Resource Geology*, 59(2):181–193.
- Yang, L.Q., Deng, J., Guo, L.N., et al., 2016a. Origin and Evolution of Ore Fluid, and Gold-Deposition Processes at the Giant Taishang Gold Deposit, Jiaodong Peninsula, Eastern China. *Ore Geology Reviews*, 72: 585–602. <https://doi.org/10.1016/j.oregeorev.2015.08.021>
- Yang, L.Q., Deng, J., Wang, Z.L., et al., 2016b. Thermochronologic Constraints on Evolution of the Linglong Metamorphic Core Complex and Implications for Gold Mineralization: A Case Study from the Xiadian Gold Deposit, Jiaodong Peninsula, Eastern China. *Ore Geology Reviews*, 72:165–178. <https://doi.org/10.1016/j.oregeorev.2015.07.006>
- Yang, L.Q., Deng, J., Wang, Z.L., et al., 2016c. Relationships between Gold and Pyrite at the Xincheng Gold Deposit, Jiaodong Peninsula, China: Implications for Gold Source and Deposition in a Brittle Epizonal Environment. *Economic Geology*, 111(1): 105–126. <https://doi.org/10.2113/econgeo.111.1.105>
- Yang, L.Y., Yang, L.Q., Yuan, W.M., et al., 2013. Origin and Evolution of Ore Fluid for Orogenic Gold Traced by D-O Isotopes: A Case from the Jiapigou Gold Belt, China. *Acta Petrologica Sinica*, 29(11):4025–4035.
- Yang, Q.Y., Santosh, M., 2015. Paleoproterozoic Arc Magmatism in the North China Craton: No Siderian Global Plate Tectonic Shutdown. *Gondwana Research*, 28(1): 82–105.
- Yang, Z.S., Hou, Z.Q., Meng, X.J., et al., 2009b. Post-Collisional Sb and Au Mineralization Related to the South Tibetan Detachment System, Himalayan Orogen. *Ore Geology Reviews*, 36(1–3):194–212.
- Yasuhara, H., Polak, A., Mitani, Y., et al., 2006. Evolution of Fracture Permeability through Fluid-Rock Reaction under Hydrothermal Conditions. *Earth and Planetary Science Letters*, 244(1–2):186–200.
- Zhai, M.G., Peng, P., 2007. Paleoproterozoic Events in the North China Craton. *Acta Petrologica Sinica*, 23(11): 2665–2682 (in Chinese with English abstract).
- Zhai, W., Sun, X.M., Yi, J.Z., et al., 2014. Geology, Geochemistry, and Genesis of Orogenic Gold-Antimony Mineralization in the Himalayan Orogen, South Tibet, China. *Ore Geology Reviews*, 58: 68–90. <https://doi.org/10.1016/j.oregeorev.2013.11.001>
- Zhai, Y.S., Wang, J.P., Peng, R.M., et al., 2009. Research on Superimposed Metallogenic Systems and Polygenetic

- Mineral Deposits. *Earth Science Frontiers*, 16(6): 282—290 (in Chinese with English abstract).
- Zhang, G. Y., Zheng, Y. Y., Zhang, J. F., et al., 2011. Ore-Control Structural and Geochronologic Constrains in Shalagang Antimony Deposit in Southern Tibet, China. *Acta Petrologica Sinica*, 27(7): 2143—2149 (in Chinese with English abstract).
- Zhang, H. F., Parrish, R., Zhang, L., et al., 2007. A-Type Granite and Adakitic Magmatism Association in Songpan-Garze Fold Belt, Eastern Tibetan Plateau: Implication for Lithospheric Delamination. *Lithos*, 97(3—4): 323—335. <https://doi.org/10.1016/j.lithos.2007.01.002>
- Zhang, L., Chen, H. Y., Chen, Y. J., et al., 2012. Geology and Fluid Evolution of the Wangfeng Orogenic-Type Gold Deposit, Western Tian Shan, China. *Ore Geology Reviews*, 49: 85—95. <https://doi.org/10.1016/j.oregeorv.2012.09.002>
- Zhang, L. C., Shen, Y. C., Ji, J. S., 2003. Characteristics and Genesis of Kanggur Gold Deposit in the Eastern Tian-shan Mountains, NW China: Evidence from Geology, Isotope Distribution and Chronology. *Ore Geology Reviews*, 23(1—2): 71—90. [https://doi.org/10.1016/s0169-1368\(03\)00016-7](https://doi.org/10.1016/s0169-1368(03)00016-7)
- Zhang, L. C., Zhou, X. H., Ding, S. J., 2008. Mantle-Derived Fluids Involved in Large-Scale Gold Mineralization, Jiadong District, China: Constraints Provided by the He-Ar and H-O Isotopic Systems. *International Geology Review*, 50(5): 472—482. <https://doi.org/10.2747/0020-6814.50.5.472>
- Zhao, H. S., Wang, Q. F., Groves, D. I., et al., 2019. A Rare Phanerozoic Amphibolite-Hosted Gold Deposit at Danba, Yangtze Craton, China: Significance to Fluid and Metal Sources for Orogenic Gold Systems. *Mineralium Deposita*, 54(1): 133—152. <https://doi.org/10.1007/s00126-018-0845-x>
- Zhong, R. C., Brugger, J., Tomkins, A. G., et al., 2015. Fate of Gold and Base Metals during Metamorphic Devolatilization of a Pelite. *Geochimica et Cosmochimica Acta*, 171: 338—352. [doi:10.1016/j.gca.2015.09.013](https://doi.org/10.1016/j.gca.2015.09.013)
- Zhou, M. F., Yan, D. P., Kennedy, A. K., et al., 2002a. SHRIMP U-Pb Zircon Geochronological and Geochemical Evidence for Neoproterozoic Arc-Magmatism along the Western Margin of the Yangtze Block, South China. *Earth and Planetary Science Letters*, 196(1—2): 51—67. [https://doi.org/10.1016/s0012-821x\(01\)00595-7](https://doi.org/10.1016/s0012-821x(01)00595-7)
- Zhou, T. H., Goldfarb, R. J., Phillips, N. G., 2002b. Tectonics and Distribution of Gold Deposits in China: An Overview. *Mineralium Deposita*, 37(3): 249—282.
- Zhou, M. F., Yan, D. P., Vasconcelos, P. M., et al., 2008. Structural and Geochronological Constraints on the Tectono-Thermal Evolution of the Danba Domal Terrane, Eastern Margin of the Tibetan Plateau. *Journal of Asian Earth Sciences*, 33(5—6): 414—427. <https://doi.org/10.1016/j.jseae.2008.03.003>
- Zhu, L. H., Qi, X. X., Peng, S. B., Li, Z. Q., 2011. Evolution of Ore Forming Fluid of Daping Gold Deposit in Ailaoshan Tectonic Zone, Southeast Tibet. *Acta Petrologica Sinica*, 27(11): 3395—3408.
- Zhu, Y. N., Peng, J. T., 2015. Infrared Microthermometric and Noble Gas Isotope Study of Fluid Inclusions in Ore Minerals at the Woxi Orogenic Au-Sb-W Deposit, Western Hunan, South China. *Ore Geology Reviews*, 65: 55—69. <https://doi.org/10.1016/j.oregeorev.2014.08.014>

附中文参考文献

- 毕献武, 胡瑞忠, 何明友, 1997. 哀牢山金矿带主要金矿床成矿流体特征. *矿物学报*, 17(4): 435—441.
- 陈衍景, Pirajno, F., 赖勇, 等, 2004. 胶东矿集区大规模成矿时间和构造环境. *岩石学报*, 20(4): 907—922.
- 陈衍景, 翟明国, 蒋少涌, 2009. 华北大陆边缘造山过程与成矿研究的重要进展和问题. *岩石学报*, 25(11): 2695—2726.
- 邓军, 杨立强, 王长明, 2011. 三江特提斯复合造山与成矿作用研究进展. *岩石学报*, 27(9): 2501—2509.
- 李华健, 王庆飞, 杨林, 等, 2017. 青藏高原碰撞造山背景造山型金矿床: 构造背景、地质及地球化学特征. *岩石学报*, 33(7): 2189—2201.
- 李士辉, 张静, 邓军, 等, 2011. 哀牢山南段长安金矿床成矿流体特征及成因类型探讨. *岩石学报*, 27(12): 3777—3786.
- 梁业恒, 孙晓明, 石贵勇, 等, 2011. 云南哀牢山老王寨大型造山型金矿成矿流体地球化学. *岩石学报*, 27(9): 2533—2540.
- 毛景文, 谢桂青, 李晓峰, 等, 2004. 华南地区中生代大规模成矿作用与岩石圈多阶段伸展. *地学前缘*, 11(1): 45—55.
- 毛景文, 谢桂青, 张作衡, 等, 2005. 中国北方中生代大规模成矿作用的期次及其地球动力学背景. *岩石学报*, 21(1): 169—188.
- 王学明, 邵世才, 汪东波, 等, 2000. 西秦岭金矿床包裹体、氢氧同位素特征及其地质意义. *贵金属地质*, 9(1): 44—48.
- 翟明国, 彭澎, 2007. 华北克拉通古元古代构造事件. *岩石学报*, 23(11): 2665—2682.
- 翟裕生, 王建平, 彭润民, 等, 2009. 叠加成矿系统与多成因矿床研究. *地学前缘*, 16(6): 282—290.
- 张刚阳, 郑有业, 张建芳, 等, 2011. 西藏沙拉岗梯矿控矿构造及成矿时代约束. *岩石学报*, 27(7): 2143—2149.